

# RORL: Robust Offline Reinforcement Learning via Conservative Smoothing

Rui Yang<sup>1\*</sup>, Chenjia Bai<sup>2\*</sup>, Xiaoteng Ma<sup>1</sup>, Zhaoran Wang<sup>3</sup>, Chongjie Zhang<sup>1</sup>, Lei Han<sup>4</sup>

<sup>1</sup>Tsinghua University, <sup>2</sup>Harbin Institute of Technology

<sup>3</sup>Northwestern University, <sup>4</sup>Tencent Robotics X

yangrui19@mails.tsinghua.edu.cn, baichenjia255@gmail.com

ma-xt17@mails.tsinghua.edu.cn, zhaoranwang@gmail.com

chongjie@tsinghua.edu.cn, lxhan@tencent.com

## Abstract

Offline reinforcement learning (RL) provides a promising direction to exploit the massive amount of offline data for complex decision-making tasks. Due to the distribution shift issue, current offline RL algorithms are generally designed to be conservative for value estimation and action selection. However, such conservatism impairs the robustness of learned policies, leading to a significant change even for a small perturbation on observations. To trade off robustness and conservatism, we propose Robust Offline Reinforcement Learning (RORL) with a novel conservative smoothing technique. In RORL, we explicitly introduce regularization on the policy and the value function for states near the dataset and additional conservative value estimation on these OOD states. Theoretically, we show RORL enjoys a tighter suboptimality bound than recent theoretical results in linear MDPs. We demonstrate that RORL can achieve the state-of-the-art performance on the general offline RL benchmark and is considerably robust to adversarial observation perturbation.

## 1 Introduction

Over the past few years, deep reinforcement learning (RL) has been a vital tool for various decision-making tasks [31, 44, 42, 9] in a trial-and-error manner. A major limitation of current deep RL algorithms is that they require intense online interactions with the environment [27]. These data collecting processes can be costly and even prohibitive in many real-world scenarios such as robotics and health care. Offline RL [13, 25] is gaining more attention recently since it offers probabilities to learn reinforced decision-making strategies from fully offline datasets.

The main challenge of offline RL is the distribution shift between the offline dataset and the learned policy, which would lead to significant overestimation for the out-of-distribution (OOD) actions [13, 25]. To overcome such an issue, a series of offline RL works [51, 13, 59, 26, 2, 4] propose to celebrate conservatism, such as constraining the learned policy close to supported distribution or penalizing the  $Q$ -values of OOD actions. In addition, another stream of works builds upon model-based offline RL algorithms [62, 61, 50], which leverages the ensemble dynamics models to enforce pessimism via uncertainty penalizing or data generation.

However, conservatism is not the only concern when applying offline RL to the real world. Due to the sensor errors and model mismatch, the robustness of offline RL is crucial under the realistic engineering conditions, which has not been well studied yet. In online RL, a series of works have been studied to learn the optimal policy under worst-case perturbations of the observation [63, 36, 18] or environmental dynamics [49, 38, 39]. Yet, it is non-trivial to apply online robust RL techniques

---

\*Equal Contribution

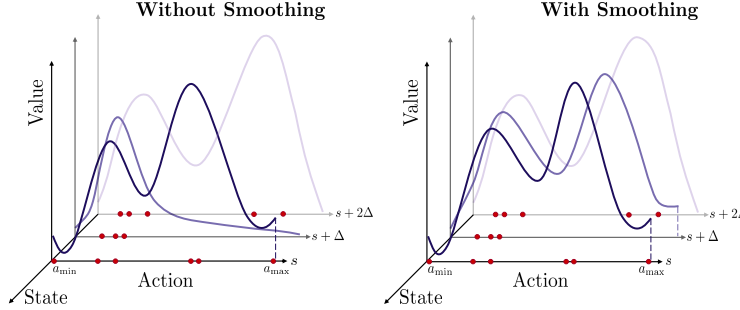


Figure 1: A schematic diagram of RORL. The red spots represent the offline data samples. Without state smoothing, the value function would change drastically over neighbor states and induce an unstable policy. Yet, the smoothness may also lead to value overestimation of dangerous areas. RORL trades off smoothness and possible overestimation as discussed in Sec 4.

into the offline problems. The main challenge is that the perturbation of either states or actions may bring OOD data and extra overestimation for the value function. New techniques are needed to tackle the conservatism and robustness simultaneously in the offline RL.

This paper studies robust offline RL against adversarial observation perturbation, where the agent needs to learn the policy conservatively while handling the potential OOD observation with perturbation. We first demonstrate that current value-based offline RL algorithms lack the necessary smoothness for the policy, which is visualized in Figure 1. As an illustration, we show that a famous baseline method CQL [26] learns a non-smooth value function, leading to significant performance degradation for even a tiny scale perturbation on observation (see Section 3 for details). Notice that simply adopting the smoothing technique for existing methods may result in extra overestimation at the boundary of supported distribution and lead the agent toward the unsafe areas.

To this end, we propose Robust Offline Reinforcement Learning (RORL) with a novel conservative smoothing technique, which explicitly handles the overestimation of OOD state-action pairs. Specifically, we explicitly introduce smooth regularization on both the values and policies for states near the dataset support and conservatively estimate the values of these OOD states based on pessimistic bootstrapping. In addition, we theoretically prove that RORL yields a valid uncertainty quantifier in linear MDPs and enjoys a tighter suboptimality bound than previous work [4].

In our experiments, we demonstrate that RORL can achieve state-of-the-art (SOTA) performance in D4RL benchmark [10] for offline RL given a suitable adversarial perturbation scale during training. The surprising performance in the benchmark shows that the robust training improves the generalization ability and leads to performance improvement even in non-perturbed tasks. Meanwhile, compared with the current SOTA baseline [2], RORL is considerably more robust to adversarial perturbations on observations. We conduct the ablation study under different types of adversarial attacks on the observations, showing the consistently superior performance over several tasks.

## 2 Preliminaries

**Offline RL and PBRL** Considering an episodic MDP  $\mathcal{M} = (\mathcal{S}, \mathcal{A}, T, r, \gamma, \mathbb{P})$ , where  $\mathcal{S}$  is the state space,  $\mathcal{A}$  is the action space,  $T$  is the length of the episode,  $r$  is the reward function,  $\mathbb{P}$  is the dynamics, and  $\gamma$  is the discount factor. In offline RL, the objective of the agent is to find an optimal policy by sampling experience from a fixed dataset  $\mathcal{D} = \{(s_t^i, a_t^i, r_t^i, s_{t+1}^i)\}$ . Nevertheless, directly applying off-policy algorithms in offline RL has distribution shift problem. In  $Q$ -learning, the value function evaluated on the greedy action  $a'$  in Bellman operator  $\mathcal{T}Q = r + \gamma \mathbb{E}_{s'}[\max_{a'}(s', a')]$  tends to have extrapolation error since  $(s', a')$  has barely occurred in  $\mathcal{D}$ . There are mainly three kinds of methods to track the distribution shift problem in offline RL, including policy constraints, conservative value function, and uncertainty-based methods.

Pessimistic Bootstrapping for Offline RL (PBRL) [4] is an uncertainty-based method that uses bootstrapped  $Q$ -functions for uncertainty quantification and OOD sampling for regularization. Specifically, PBRL maintains  $K$  bootstrapped  $Q$  functions to quantify the epistemic uncertainty and performs pessimistic update to penalize  $Q$  functions with large uncertainties. The uncertainty is defined as

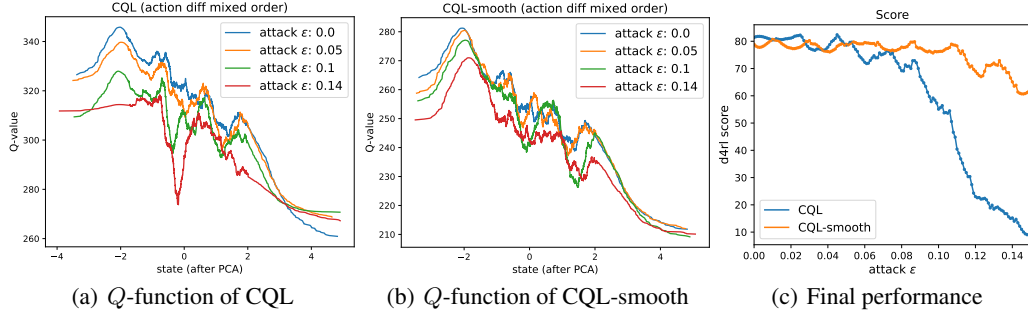


Figure 2: Figure (a) and (b) illustrate the  $Q$ -functions of  $\hat{s}$  with adversarial noises in CQL and CQL-smooth, respectively. The same moving average factor is used in plotting both figures. Figure (c) shows the performance evaluation of CQL and CQL-smooth with different perturbation scale. We use 100 different  $\epsilon \in [0.0, 0.15]$  for the evaluation.

the standard deviation among bootstrapped  $Q$ -functions. For each bootstrapped  $Q$ -function, the Bellman target is defined as  $\hat{T}Q(s, a) = r(s, a) + \gamma \mathbb{E}_{s' \sim P(\cdot|s, a), a' \sim \pi(\cdot|s')} [Q(s', a') - \beta u(s', a')]$ . Under linear MDP assumptions, this uncertainty is equivalent to the LCB penalty and is provably efficient [22]. Furthermore, PBRL incorporates OOD sampling in training by sampling OOD actions to form  $(s, a^{\text{ood}})$  pairs, where  $a^{\text{ood}}$  follows the learned policy. The learning target for  $(s, a^{\text{ood}})$  is  $\hat{T}^{\text{ood}}Q(s, a^{\text{ood}}) := Q(s, a^{\text{ood}}) - \beta u(s, a^{\text{ood}})$ , which introduces uncertainty penalization to enforce pessimistic  $Q$ -functions for OOD actions.

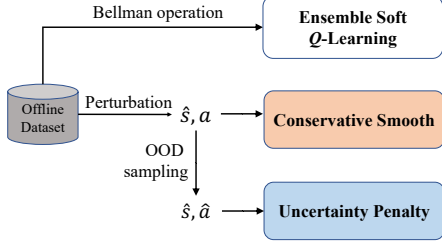
**Smooth Regularized RL** Robust RL aims to learn a robust policy against the adversarial perturbed environment in online RL. SR<sup>2</sup>L [43] enforces smoothness in both the policy and  $Q$ -functions. Specifically, SR<sup>2</sup>L encourages the outputs of the policy and value function to not change much when injecting small perturbation to the state. For state  $s$ , SR<sup>2</sup>L constructs a perturbation set  $\mathbb{B}_d(s, \epsilon) = \{\hat{s} : d(s, \hat{s}) \leq \epsilon\}$  and introduces a smoothness regularizer for policy as  $\mathcal{R}_s^\pi = \mathbb{E}_{s \sim \rho^\pi} \max_{\hat{s} \in \mathbb{B}_d(s, \epsilon)} \mathcal{D}(\pi(\cdot|s) \parallel \pi(\cdot|\hat{s}))$ , where  $\mathcal{D}(\cdot \parallel \cdot)$  is a distance metric and the max operator gives an adversarial manner to choose  $\hat{s}$ . Similarly, the smoothness regularizer for the value function is defined as  $\mathcal{R}_s^V = \mathbb{E}_{s \sim \rho^\pi, a \sim \pi} \max_{\hat{s} \in \mathbb{B}_d(s, \epsilon)} (Q(s, a) - Q(\hat{s}, a))^2$ . The induced smoothness is shown to improve robustness against both random and adversarial perturbations.

### 3 Robustness of Offline RL: A Motivating Example

We give a motivating example to illustrate the robustness of the popular CQL [26] policies. We introduce an adversarial attack on state  $s$  to obtain  $\hat{s} = \arg \max_{\hat{s} \in \mathbb{B}_d(s, \epsilon)} D_J(\pi_\theta(\cdot|s) \parallel \pi_\theta(\cdot|\hat{s}))$ , where  $\mathbb{B}_d$  is the perturbation set to ensure  $d(s, \hat{s}) \leq \epsilon$  and the Jeffrey's divergence  $D_J$  for two distributions  $P, Q$  is defined by:  $D_J(P \parallel Q) = \frac{1}{2} [D_{\text{KL}}(P \parallel Q) + D_{\text{KL}}(Q \parallel P)]$ . To obtain  $\hat{s}$ , we take gradient ascent with respect to the loss function  $D_J(\pi_\theta(\cdot|s) \parallel \pi_\theta(\cdot|\hat{s}))$  and restrict the outputs to the  $\mathbb{B}_d(s, \epsilon)$  set, where  $\pi_\theta$  is a learned CQL policy and  $\epsilon$  controls the strength of attack.

In the *walker-medium-v2* task from D4RL [10], we use various setups of  $\epsilon$  for adversarial attack to evaluate the robustness of CQL policies. Specifically, we use  $\epsilon \in \{0, 0.05, 0.1, 0.14\}$  to control the strengths of the attack, where we have  $\hat{s} = s$  if  $\epsilon = 0$ . Given a specific  $\epsilon$ , we sample  $N$  state-action pairs  $\{(s_i, a_i)\}$  from the offline dataset, and then perform adversarial attack to obtain  $\{(\hat{s}_i, a_i)\}$  and also the corresponding  $Q$ -values  $\{Q_i(\hat{s}_i, a_i)\}$ , where the  $Q$ -function is the trained CQL critic.

Figure 2(a) shows the relationship between  $\hat{s}_i$  and the corresponding  $Q_i$  with different  $\epsilon$ . To visualize  $\hat{s}_i$ , we perform PCA dimensional reduction [47] and choose one of the reduced dimensions to represent  $\hat{s}_i$ . With the increase of  $\epsilon$  in the adversarial attack, the  $Q$ -curve has greater deviation compared to the curve with  $\epsilon = 0$ . The result signifies that the  $Q$ -function of CQL is not smooth in state space, which makes the adversarial noises easily affect the  $Q$ -function. As a comparison, we apply the proposed conservative smoothing loss in CQL training (i.e., *CQL-smooth*) and use the same evaluation method to obtain  $\hat{s}_i$  and  $Q_i$ . According to the result in Figure 2(b), the value function becomes smoother.




---

**Algorithm 1: RORL**


---

**while not converged do**

Sample mini-batch transitions  $(s, a, r, s')$  from  $\mathcal{D}$ .  
 Perform extended soft  $Q$ -learning to train multiple  $Q$ -functions  $\{Q_1, \dots, Q_K\}$ .  
 Sample  $\hat{s}$  from  $\mathbb{B}_d(s, \epsilon)$  to obtain  $(\hat{s}, a)$  pairs.  
 Perform adversarial smoothing for the  $Q$ -network.  
 Calculate uncertainty to penalize  $(\hat{s}, \hat{a})$  for conservatism.  
 Combining terms to train the critic with Eq. (5).  
 Train the policy with smooth constraint as Eq. (6).

---

Figure 3: **RORL Algorithm:** RORL trains multiple soft  $Q$ -functions for uncertainty quantification. The conservative smoothing loss is calculated for  $(\hat{s}, a)$  with perturbed state. We perform uncertainty penalization for  $(\hat{s}, \hat{a})$  with OOD actions.

In addition, we show how the adversarial attack affects the final performance of offline RL policies. We use  $\epsilon \in [0, 0.15]$  to evaluate both the original CQL policies (i.e., *CQL*) and CQL with conservative smoothing loss (i.e., *CQL-smooth*) in adversarial attack. Figure 2(c) shows the performance with different settings of  $\epsilon$ . We find that our smooth constraints significantly improve the robustness of CQL, especially for large adversarial noises.

## 4 Robust Offline RL via Conservative Smoothing

In RORL, we develop smooth regularization on both the policy and the value function for states near the dataset. The smooth constraints make the policy and  $Q$ -function robust to perturbation in the dataset (for offline training) and interactive samples (for online evaluation). Nevertheless, the smoothness may lead to value overestimation of the edge of the supported dataset. To address this problem, we adopt bootstrapped  $Q$ -functions [34] for uncertainty quantification and sample OOD actions for penalization. RORL obtains conservative and smooth value estimation on both OOD states and actions, which improves the generalization ability of offline RL algorithms. The overall architecture of RORL is given in Figure 3.

**Robust  $Q$ -function** We sample three sets of state-action pairs and apply different loss functions to obtain a conservative smooth policy. Specifically, for a  $(s, a)$  pair sampled from  $\mathcal{D}$ , we construct a perturbation set  $\mathbb{B}_d(s, \epsilon)$  to obtain  $(\hat{s}, a)$  pairs, where  $\hat{s} \in \mathbb{B}_d(s, \epsilon)$  and  $\epsilon$ . Then we perform OOD sampling by using the current policy  $\pi_\theta$  to obtain  $(\hat{s}, \hat{a})$  pairs, where  $\hat{a} \sim \pi_\theta(\hat{s})$ . RORL contains  $K$   $Q$ -functions trained by Soft  $Q$ -learning as critics. We denote the parameters of  $i$ -th  $Q$ -function and the target  $Q$ -function as  $\phi_i$  and  $\phi'_i$ , respectively. In the following, we give different learning targets for  $(s, a)$ ,  $(\hat{s}, a)$ , and  $(\hat{s}, \hat{a})$  pairs, respectively.

First, for a  $(s, a)$  pair sampled from  $\mathcal{D}$ , we apply extended soft  $Q$ -learning to obtain the target as

$$\hat{T}Q_{\phi_i}(s, a) := r(s, a) + \gamma \mathbb{E}_{a' \sim \pi_\theta(\cdot|s)} \left[ \min_{j=1, \dots, K} Q_{\phi'_j}(s', a') - c \cdot \log \pi_\theta(a'|s') \right], \quad (1)$$

where the next- $Q$  function takes minimum value among the target  $Q$ -functions.

Then, for a  $(\hat{s}, a)$  pair with a perturbed state, we enforce smoothness in  $Q$ -function by minimizing the  $Q$ -value difference between  $Q(s, a)$  and  $Q(\hat{s}, a)$ . In particular, we choose an adversarial  $\hat{s} \in \mathbb{B}_d(s, \epsilon)$  that maximizes  $\mathcal{L}(Q(\hat{s}, a), Q(s, a))$ , and then minimize this loss function with the adversarial  $\hat{s}$ , where  $\mathcal{L}$  is a distance measure. Intuitively, we want that the  $Q$ -function is smooth with the most difficult (i.e., adversarial) attack in  $\mathbb{B}_d(s, \epsilon)$ , where  $\epsilon$  controls the perturbation scale. To solve such a min-max problem, we maximize  $\mathcal{L}(Q(\hat{s}, a), Q(s, a))$  to obtain  $\hat{s}$ , and then minimize the loss function with the selected  $\hat{s}$ .

$$\mathcal{L}_{\text{smooth}}(s, a; \phi_i) = \max_{\hat{s} \in \mathbb{B}_d(s, \epsilon)} \mathcal{L}(Q_{\phi_i}(\hat{s}, a), Q_{\phi_i}(s, a)) \quad (2)$$

where  $\mathcal{L}(\cdot, \cdot)$  is the smooth loss function, and we denote  $\delta(s, \hat{s}, a) = Q_{\phi_i}(\hat{s}, a) - Q_{\phi_i}(s, a)$ . We remark that if  $\delta(s, \hat{s}, a) > 0$ , the perturbed state may induce an overestimated  $Q$ -value that we need to smooth. In contrast, if  $\delta(s, \hat{s}, a) < 0$ , the perturbed  $Q$ -function is underestimated, which does

not cause a serious problem in offline RL. As a result, we use different weights for  $\delta(s, \hat{s}, a)_+$  and  $\delta(s, \hat{s}, a)_-$ . The definition of  $\mathcal{L}(\cdot, \cdot)$  is give as follows,

$$\mathcal{L}(Q_{\phi_i}(\hat{s}, a), Q_{\phi_i}(s, a)) = (1 - \tau)\delta(s, \hat{s}, a)_+^2 + \tau\delta(s, \hat{s}, a)_-^2, \quad (3)$$

where we choose  $\tau \leq 0.5$ ,  $x_+ = \max(x, 0)$  and  $x_- = \min(x, 0)$ . In this term, we does not introduce OOD action  $\hat{a}$  for smoothing since the actions are desired to be close to the behavior actions in the dataset for areas near the offline data.

Finally, to prevent overestimation of OOD states and actions, we use bootstrapped uncertainty  $u(\hat{s}, \hat{a})$  as a penalty for  $Q(\hat{s}, \hat{a})$ , where  $\hat{a} \sim \pi(\hat{s})$  is an OOD action sampled from the current policy  $\pi$ . We remark that a similar OOD sampling is also used in PBRL [4]. *The difference is that PBRL only penalizes the OOD actions, while RORL penalizes both the OOD states and actions to provide conservatism for unfamiliar areas.* The ensemble technique in RL comes from Bootstrapped DQN [34]. The ensemble forms an estimation of the  $Q$ -posterior, which yields diverse predictions on areas with scarce data.  $u(\hat{s}, \hat{a})$  quantifies the deviation of a datapoint from the offline dataset [2, 4]. We follow PBRL and use a loss function as:

$$\mathcal{L}_{\text{ood}}(s; \phi_i) = \mathbb{E}_{\hat{s} \sim \mathbb{B}_d(s, \epsilon), \hat{a} \sim \pi_\theta(\hat{s})} (\hat{\mathcal{T}}_{\text{ood}} Q_{\phi_i}(\hat{s}, \hat{a}) - Q_{\phi_i}(\hat{s}, \hat{a}))^2, \quad (4)$$

where the pseudo-target for the OOD datapoints is computed as:  $\hat{\mathcal{T}}_{\text{ood}} Q_{\phi_i}(\hat{s}, \hat{a}) := Q_{\phi_i}(\hat{s}, \hat{a}) - u(\hat{s}, \hat{a})$ , where  $u(\hat{s}, \hat{a}) := \sqrt{\frac{1}{K} \sum_{k=1}^K (Q_{\phi_k}(\hat{s}, \hat{a}) - \bar{Q}_\phi(\hat{s}, \hat{a}))^2}$ . The bootstrapped uncertainty  $u(\hat{s}, \hat{a})$  is defined as the standard deviation among the  $Q$ -ensemble.

Combining the loss functions above, RORL has the following loss function for each  $Q_{\phi_i}$ :

$$\min_{\phi_i} \mathbb{E}_{s, a, r, s' \sim \mathcal{D}} \left[ (\hat{\mathcal{T}} Q_{\phi_i}(s, a) - Q_{\phi_i}(s, a))^2 + \alpha \mathcal{L}_{\text{smooth}}(s, a; \phi_i) + \beta \mathcal{L}_{\text{ood}}(s; \phi_i) \right], \quad (5)$$

**Robust Policy** We learn a robust policy by using a smooth constraint to make the policy change less with perturbations. Similarly, we choose an adversarial state  $\hat{s} \in \mathbb{B}_d(s, \epsilon)$  that maximizes  $D_J(\pi_\theta(\cdot|s) \parallel \pi_\theta(\cdot|\hat{s}))$ , and then minimize the policy difference between  $\pi_\theta(\cdot|s)$  and  $\pi_\theta(\cdot|\hat{s})$ . To conclude, we minimize the following loss function for the policy,

$$\min_{\theta} \left[ \mathbb{E}_{s, a, r, s' \sim \mathcal{D}} \left[ - \min_{j=1, \dots, K} Q_{\phi_j}(s, a) + \alpha_2 \max_{\hat{s} \in \mathbb{B}_d(s, \epsilon)} D_J(\pi_\theta(\cdot|s) \parallel \pi_\theta(\cdot|\hat{s})) + c \log \pi_\theta(a|s) \right] \right]. \quad (6)$$

where the first term aims to maximize the minimum of the ensemble  $Q$ -functions to obtain a conservative policy, and the third term is regularization of entropy.

## 5 Theoretical Analysis

We analyze the simplified learning objective of RORL in linear MDPs [21, 22], where the feature map of the state-action pair takes the form of  $\phi : \mathcal{S} \times \mathcal{A} \rightarrow \mathbb{R}^d$ , and the transition kernel and the reward function are assumed to be linear in  $\phi$ . The parameter  $\tilde{w}_t$  of RORL can be solved in closed form following the least squares value iteration algorithm (LSVI), which minimizes the following loss function.

$$\begin{aligned} \tilde{w}_t^i = \min_{w \in \mathcal{R}^d} & \left[ \sum_{i=1}^m (y_t^i - Q_w(s_t^i, a_t^i))^2 + \sum_{i=1}^m \frac{1}{|\mathbb{B}_d(s_t^i, \epsilon)|} \sum_{\hat{s}_t^i \in \mathcal{D}_{\text{ood}}(s_t^i)} (Q_w(s_t^i, a_t^i) - Q_w(\hat{s}_t^i, a_t^i))^2 + \right. \\ & \left. \sum_{(\hat{s}, \hat{a}, \hat{y}) \sim \mathcal{D}_{\text{ood}}} (\hat{y} - Q_w(\hat{s}, \hat{a}))^2 \right], \end{aligned} \quad (7)$$

where we have  $Q_w(s_t^i, a_t^i) = \phi(s_t^i, a_t^i)^\top w$  since the  $Q$ -function is also linear in  $\phi$ . The first term in Eq. (7) is the ordinary TD-error, where we consider the setting of  $\gamma = 1$  and the  $Q$ -target is  $y_t^i = r(s_t^i, a_t^i) + V_{t+1}(s_{t+1}^i)$ . The second term is the proposed conservative smoothing loss. Specifically,  $\hat{s}_t^i \sim \mathcal{D}_{\text{ood}}(s_t^i)$  are sampled from a  $l_\infty$  ball of center  $s_t^i$  and norm  $\epsilon > 0$ , which can be formulated as  $\hat{s} \sim \mathbb{B}_d(s_t^i, \epsilon)$ . The third term is the additional OOD-sampling loss [4], which enforces conservatism for OOD actions. Differently, we use perturbed states sampled from  $\mathcal{D}_{\text{ood}} = \bigcup_{i=1}^m \mathcal{D}_{\text{ood}}(s_t^i)$

rather than states from dataset in PBRL. The OOD action  $\hat{a}$  is sampled from policy  $\pi$ . The explicit solution of Eq. (7) takes the following form by following LSVI:

$$\tilde{w}_t^i = \tilde{\Lambda}_t^{-1} \left( \sum_{i=1}^m \phi(s_t^i, a_t^i) y_t^i + \sum_{(\hat{s}, \hat{a}, \hat{y}) \sim \mathcal{D}_{\text{ood}}} \phi(\hat{s}, \hat{a}) \hat{y} \right), \quad (8)$$

where the covariance matrix  $\tilde{\Lambda}_t$  is defined as

$$\begin{aligned} \tilde{\Lambda}_t = & \sum_{i=1}^m \phi(s_t^i, a_t^i) \phi(s_t^i, a_t^i)^\top + \sum_{(\hat{s}, \hat{a}) \sim \mathcal{D}_{\text{ood}}} \phi(\hat{s}, \hat{a}) \phi(\hat{s}, \hat{a})^\top \\ & + \sum_{i=1}^m \frac{1}{|\mathbb{B}_d(s_t^i, \epsilon)|} \sum_{\hat{s}_t^i \sim \mathcal{D}_{\text{ood}}(s_t^i)} [\phi(\hat{s}_t^i, a_t^i) - \phi(s_t^i, a_t^i)] [\phi(\hat{s}_t^i, a_t^i) - \phi(s_t^i, a_t^i)]^\top. \end{aligned} \quad (9)$$

We denote the first term and the second term as  $\tilde{\Lambda}_t^{\text{in}}$  and  $\tilde{\Lambda}_t^{\text{ood}}$ , which represent the covariance matrices induced by the offline samples and OOD samples, respectively. Nevertheless, in linear MDPs, it is difficult to ensure the covariance  $\tilde{\Lambda}_t^{\text{in}} + \tilde{\Lambda}_t^{\text{ood}} \succeq \lambda I$ , since it requires that the embeddings of the samples are isotropic to make the eigenvalues of the corresponding covariance matrix lower bounded. This condition holds if we can sample embeddings uniformly from the whole embedding space. However, since the offline dataset has limited coverage in the state-action space and the OOD samples come from a limited  $l_\infty$ -ball around the offline data,  $\tilde{\Lambda}_t^{\text{in}} + \tilde{\Lambda}_t^{\text{ood}}$  cannot be guaranteed to be positive definite. PBRL [4] uses the assumption of  $\tilde{\Lambda}_t^{\text{ood}} \succeq \lambda I$ , while it is unachievable empirically. In RORL, we solve this problem by introducing an additional conservative smoothing loss, which induces a covariance matrix as  $\tilde{\Lambda}_t^{\text{ood-diff}} = \sum_{i=1}^m \frac{1}{|\mathbb{B}_d(s_t^i, \epsilon)|} \sum_{\hat{s}_t^i \sim \mathcal{D}_{\text{ood}}(s_t^i)} [\phi(\hat{s}_t^i, a_t^i) - \phi(s_t^i, a_t^i)] [\phi(\hat{s}_t^i, a_t^i) - \phi(s_t^i, a_t^i)]^\top$  (i.e., the third term in Eq. (9)). The following theorem gives the guarantees of  $\tilde{\Lambda}_t^{\text{ood-diff}} \succeq \lambda I$ .

**Theorem 1.** Assume  $\exists i \in [1, m]$  the vector group of all  $\hat{s}_t^i \sim \mathcal{D}_{\text{ood}}(s_t^i)$ :  $\{\phi(\hat{s}_t^i, a_t^i) - \phi(s_t^i, a_t^i)\}$  be full rank, then the covariance matrix  $\tilde{\Lambda}_t^{\text{ood-diff}}$  is positive-definite:  $\tilde{\Lambda}_t^{\text{ood-diff}} \succeq \lambda \cdot I$  where  $\lambda > 0$ .

Recall the covariance matrix of PBRL is  $\tilde{\Lambda}_t^{\text{PBRL}} = \tilde{\Lambda}_t^{\text{in}} + \tilde{\Lambda}_t^{\text{ood}}$ , and RORL has a covariance matrix as  $\tilde{\Lambda}_t = \tilde{\Lambda}_t^{\text{PBRL}} + \tilde{\Lambda}_t^{\text{ood-diff}}$ , we have the following corollary based on Theorem 1.

**Corollary 1.** Under the linear MDP assumptions, we have  $\tilde{\Lambda}_t \succeq \tilde{\Lambda}_t^{\text{PBRL}}$ . Further, the covariance matrix  $\tilde{\Lambda}_t$  of RORL is positive-definite:  $\tilde{\Lambda}_t \succeq \lambda \cdot I$ , where  $\lambda > 0$ .

Recent theoretical analysis shows that an appropriate uncertainty quantification is essential to provable efficiency in offline RL [22, 57, 4]. Pessimistic Value Iteration [22] defines a general  $\xi$ -uncertainty quantifier as the penalty and achieves provable efficient pessimism in offline RL. In linear MDPs, Lower Confidence Bound (LCB)-penalty [1, 21] is known to be a  $\xi$ -uncertainty quantifier for appropriately selected  $\beta_t$  as  $\Gamma^{\text{lcb}}(s_t, a_t) = \beta_t \cdot [\phi(s_t, a_t)^\top \Lambda_t^{-1} \phi(s_t, a_t)]^{1/2}$ . Following the analysis of PBRL [4], since the bootstrapped uncertainty is an estimation to the LCB-penalty and the OOD sampling provides a covariance matrix of  $\tilde{\Lambda}_t^{\text{PBRL}}$ , the proposed RORL also form a valid  $\xi$ -uncertainty quantifier with the covariance matrix  $\tilde{\Lambda}_t \succeq \lambda \cdot I$  given in Corollary 1. This allows us to further characterize the optimality gap based on the pessimistic value iteration [22, 4]. We have the following suboptimality gap under linear MDP assumptions.

**Corollary 2.**  $\text{SubOpt}(\pi^*, \hat{\pi}) \leq \sum_{t=1}^T \mathbb{E}_{\pi^*} [\Gamma_t^{\text{lcb}}(s_t, a_t)] < \sum_{t=1}^T \mathbb{E}_{\pi^*} [\Gamma_t^{\text{lcb-PBRL}}(s_t, a_t)]$ .

We refer to Appendix 9 for detailed proof. The second inequality is directly induced by  $\Gamma_t^{\text{lcb}}(s_t, a_t) < \Gamma_t^{\text{lcb-PBRL}}(s_t, a_t)$ . Therefore, RORL enjoys a tighter suboptimality bound than PBRL [4].

## 6 Experiments

We evaluate our method on D4RL benchmark [11] with various continuous-control tasks and datasets. We compare RORL with several offline RL algorithms, including (i) BC that performs behavior cloning, (ii) CQL [26] that learns conservative value function for OOD actions, (iii) EDAC [2] that

Table 1: Normalized average returns on Gym tasks, averaged over 4 random seeds. Part of the results are reported in the EDAC paper.

Task Name	BC	CQL	PBRL	SAC-10 (Reproduced)	EDAC (Paper)	RORL (Ours)
halfcheetah-random	2.2±0.0	<b>31.3±3.5</b>	11.0±5.8	<b>29.0±1.5</b>	<b>28.4±1.0</b>	<b>28.6±0.6</b>
halfcheetah-medium	43.2±0.6	46.9±0.4	57.9 ±1.5	<b>64.9±1.3</b>	<b>65.9±0.6</b>	<b>65.6±0.8</b>
halfcheetah-medium-expert	44.0±1.6	95.0±1.4	92.3±1.1	<b>107.1±2.0</b>	<b>106.3±1.9</b>	<b>107.8±0.7</b>
halfcheetah-medium-replay	37.6±2.1	45.3±0.3	45.1±8.0	<b>63.2±0.6</b>	<b>61.3±1.9</b>	<b>61.5±0.6</b>
hopper-random	3.7±0.6	5.3±0.6	26.8±9.3	<b>25.9±9.6</b>	<b>25.3±10.4</b>	<b>27.2±7.5</b>
hopper-medium	54.1±3.8	61.9±6.4	75.3±31.2	0.8±0.2	101.6±0.6	<b>105.0±0.3</b>
hopper-medium-expert	53.9±4.7	96.9±15.1	<b>110.8±0.8</b>	6.1±7.7	<b>110.7±0.1</b>	<b>112.7±0.2</b>
hopper-medium-replay	16.6±4.8	86.3±7.3	<b>100.6±1.0</b>	<b>102.9±0.9</b>	<b>101.0±0.5</b>	<b>102.1±0.4</b>
walker2d-random	1.3±0.1	5.4±1.7	8.1±4.4	1.5±1.1	16.6±7.0	<b>21.4±0.2</b>
walker2d-medium	70.9±11.0	79.5±3.2	89.6±0.7	46.7±45.3	92.5±0.8	<b>102.4±1.4</b>
walker2d-medium-expert	90.1±13.2	109.1±0.2	110.1±0.3	116.7±1.9	114.7±0.9	<b>121.2±1.5</b>
walker2d-medium-replay	20.3±9.8	76.8±10.0	77.7±14.5	<b>89.6±3.1</b>	<b>87.1±2.3</b>	<b>90.4 ± 0.5</b>
Average	36.5	61.6	67.1	54.5	<b>76.0</b>	<b>78.8</b>

learns a diversified  $Q$ -ensemble to enforce conservatism, and (iv) PBRL [4] that performs uncertainty penalization and OOD sampling. Among these methods, EDAC [2] and PBRL [4] are related to RORL since all these methods apply  $Q$ -ensemble for conservatism. EDAC needs much more  $Q$ -networks (i.e., 10~50) for hopper tasks than PBRL and RORL that use 10  $Q$ -networks. (v) We also include a basic SAC-10 algorithm as a baseline [2], which is an extension of SAC with 10  $Q$ -functions. To assign uniform adversarial attack budget on each dimension of observations, we normalize the observations for SAC-10, EDAC and RORL. More details are provided in Appendix 10.

## 6.1 Benchmark Results

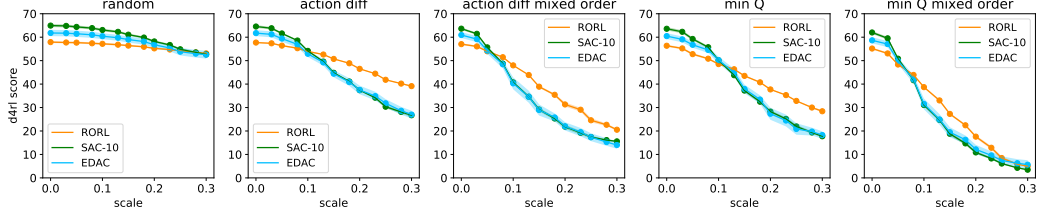
We evaluate each method on Gym domain that includes three environments (Half Cheetah, Hopper, and Walker2d) with four non-expert datasets (random, medium, medium-replay, and medium-expert). The medium-replay dataset contains experiences collected in training a medium-level policy. The random or medium dataset is generated by a single random or medium policy. The medium-expert dataset is a mixture of medium and expert datasets. We set small perturbation scale  $\epsilon$  to 0.001/0.005/0.01 for halfcheetah/hopper/walker2d tasks respectively when training RORL and do not include observation perturbation in the testing time.

Table 1 reports the performance of the average normalized score with standard deviation. (i) SAC-10 is unstable in several Walker2d and Hopper tasks since the ensemble number is relatively small to provide reliable uncertainties. (ii) EDAC solves this problem by using diversity constraints while still requiring 10~50  $Q$ -networks to obtain reasonable performance. In contrast, RORL only uses 10 ensemble  $Q$ -networks to outperform EDAC with 10~50 networks. (iii) PBRL chooses an alternative OOD-sampling technique to reduce the ensemble numbers. According to the result, RORL significantly outperforms PBRL with the same ensemble number. The reason is RORL additionally uses conservative smoothing loss for both OOD states and actions, which improves the generalization ability of the policy and  $Q$ -functions. We remark that RORL significantly improves over the current SOTA results on walker2d and hopper tasks, which might be because the two tasks require a more precise balancing of conservatism and generalization for better performance.

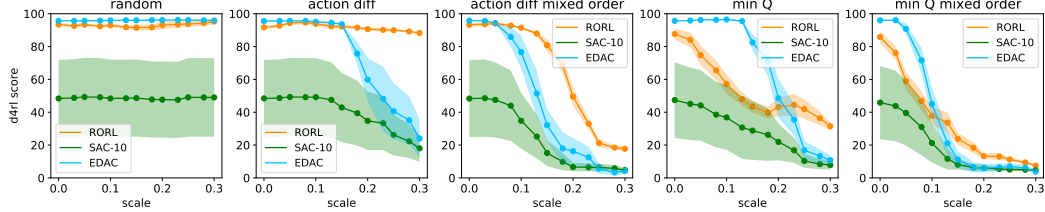
## 6.2 Adversarial Attack

We adopt three attack methods, namely *random*, *action diff*, and *min  $Q$*  following prior works [63, 38]. Given perturbation scale  $\epsilon$ , the later two methods perform adversarial perturbation on observations and are given access to the agent’s policy and value functions.

- *random* uniformly samples perturbed states in an  $l_\infty$  ball of norm  $\epsilon$ .
- *action diff* is an effective attack based on the agent’s policy and is proved to maximize an upper bound on the performance difference between perturbed and unperturbed environments [63]. It directly finds states in an  $l_\infty$  ball of norm  $\epsilon$  to minimize:  $\min_{\hat{s} \in \mathbb{B}_d(s, \epsilon)} -D_J(\pi_\theta(\cdot|s) \parallel \pi_\theta(\cdot|\hat{s}))$ .



(a) Performance under attack on halfcheetah-medium-v2 dataset



(b) Performance under attack on walker2d-medium-v2 dataset

Figure 4: Figures (a) and (b) illustrate the performance of RORL, SAC-10, and EDAC under different types of attack and attack scales range  $[0, 0.3]$ . The curves are averaged over 3 seeds and smoothed with a window size of 3. The shaded region represents half a standard deviation.

- *min Q* requires both the agent’s policy and value function to perform a relatively stronger attack. The attacker finds a perturbed state to minimize the expected return of taking an action from that state:  $\min_{\hat{s} \in \mathbb{B}_d(s, \epsilon)} Q(s, \pi_\theta(\hat{s}))$ . For ensemble-based algorithms,  $Q$  is set as the mean of ensemble  $Q$  functions.

In our experiments, the two objectives of *action diff* and *min Q* are optimized via two ways. Specifically, we optimize the objectives through:

- (1) selecting the best state from uniformly sampled 50 states, which has the advantage of simplicity and little computation cost.
- (2) uniformly sampling 20 initial states and performing gradient decent for 10 steps with a step size of  $\frac{1}{10}\epsilon$  from each initial state to find the best perturbed state. Note that we need to clip the perturbed states within the  $l_\infty$  ball at the end of each optimization step. We name this optimization method “mixed order” optimization.

We compare RORL with ensemble-based baselines EDAC and SAC-10 on halfcheetah-medium-v2 and walker2d-medium-v2 datasets. To handle large adversarial noise, we set the perturbation scale of the policy and  $Q$  functions as  $[0.1, 0.05]$  for halfcheetah-medium-v2 and  $[0.1, 0.03]$  for walker2d-medium-v2 in RORL’s training phase. More detailed description can be found in Appendix 10. The results are shown in Figure 4. In the results, RORL exhibits improved robustness than other baselines under adversarial attacks and decreases the slowest as  $\epsilon$  increases. On the other hand, we find that random attack is not effective for ensemble-based offline RL algorithms, and the “mixed order” attack brings more significant performance drop than vanilla zero-order optimization.

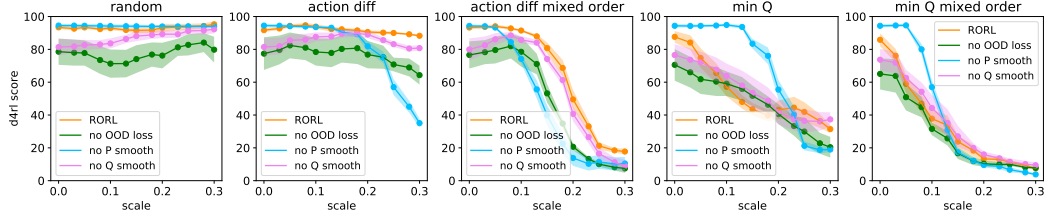


Figure 5: Ablation studies on walker2d-medium-v2 with varying perturbation scale. The curve is averaged across 3 random seeds and smoothed with a window size of 3. The shaded region represents half a standard deviation.



### 6.3 Ablations

We conducted ablation studies on walker2d-medium-v2 dataset to evaluate the importance of the policy smoothing term, the Q function smoothing term and the penalty for OOD states in Figure 5. From the results, we can conclude that each loss contributes to the performance of RORL under adversarial observation attacks. The policy smoothing loss is essential when the perturbation scale is large, while the performance of “no P smooth” is higher than RORL when the scale is smaller than 0.1. Besides, learning without OOD loss performs worse than RORL at almost all the perturbation scales. In addition, Q smooth loss has the minimal impact, which is reasonable since the basic algorithm SAC-10 is based on 10 ensemble Q networks. Our smoothing technique may have a more significant impact on baselines with fewer Q networks, such as CQL in Section 3.

## 7 Related Works

**Offline RL** Research related to offline RL has experienced explosive growth in recent years. In model-free domain, offline RL methods focus on correcting the extrapolation error [13] in the off-policy algorithms. The natural idea is to regularize the learned policy near the dataset distribution [51, 55, 32, 53, 59, 12]. For example, MARVIL reweights the policy with exponential advantage, which implicitly guarantees the policy within the KL-divergence neighborhood of the behavior policy. Another stream of model-free methods prevents the selection of OOD actions by penalizing their Q-value [25, 26, 2, 8]. With the ensemble Q networks and the additional loss term to diversify their gradients, EDAC [2] achieves SOTA performance in the D4RL benchmark. Instead of diversifying gradients, PBRL [4] proposes explicit training of the OOD actions, which achieves comparable performance with fewer ensemble networks. Inspired by EDAC and PBRL, we build our work upon ensemble networks, focusing more on smoothness over the state space.

Besides the surprising empirical results, theoretical analysis of offline reinforcement learning algorithms is of increasing interest [7, 22, 40, 57, 60]. Though the assumptions for the dataset vary in the different papers, they all suggest that pessimism and conservatism are necessary for offline RL. Our paper can be viewed as a robust extension to the previous work [22] (see Section 5 for details).

**Robust RL** The research line of robust RL can be traced back to  $H_\infty$ -control theory [56, 5], where policies are optimized to be well-performed in the worst possible deterministic environment. Depending on the definition, there are different streams of research on robust RL. As the extension of robust control to MDPs, Robust MDPs (RMDPs) [33, 19, 41, 17] are proposed to formulate the perturbation of transition probabilities for MDPs. Though some recent analyses with theoretical guarantees come out under specific assumptions for RMDP [65, 58, 28], there is currently no practical algorithm to solve RMDP in a large-scale problem, expect some linear approximation attempt [46]. In online RL, domain randomization [48, 30] assumes the model uncertainty can be predefined in data collection by changing the setup of a simulator. However, it is not practical for offline RL. Robust Adversarial Reinforcement Learning (RARL) [38] and Noisy Robust Markov Decision Process (NR-MDP) [23] study the robust RL with the perturbed actions, showing that the policy robustness to adversarial or noisy actions can also induce robustness for model parameter changes.

The most related work to ours is SR<sup>2</sup>L [43], which shows policy smoothing can lead to significant performance improvements in the online setting. In contrast, we focus on the offline setting and tackle the potential overestimation of perturbed states. Another related work is S4RL [45], where the authors study different data augmentation methods to smooth observations in offline RL. Their result supports the necessity of state smoothing. More related works are given in Appendix 12.

## 8 Conclusion

We propose Robust Offline Reinforcement Learning (RORL) to trade-off conservatism and robustness for offline RL. To achieve that, we introduce the conservative smoothing for the perturbed states while actively underestimating their values based on pessimistic bootstrapping to keep conservative. We show that RORL can achieve comparable performance with fewer ensemble Q networks than the previous methods in the offline RL benchmark. The result supports that our proposed conservative smoothing techniques benefit general offline RL by improving the generalization ability. In addition, we demonstrate that RORL is also robust to adversarial perturbations across the different types of

attacks. We hope our work can promote the application of offline RL under real-world engineering conditions.

The main limitation of our method is that the adversarial state sampling slows down the computing process, which may be improved in future work.

## References

- [1] Yasin Abbasi-Yadkori, Dávid Pál, and Csaba Szepesvári. Improved algorithms for linear stochastic bandits. In *Advances in neural information processing systems*, volume 24, pages 2312–2320, 2011.
- [2] Gaon An, Seungyong Moon, Jang-Hyun Kim, and Hyun Oh Song. Uncertainty-based offline reinforcement learning with diversified q-ensemble. *Advances in Neural Information Processing Systems*, 34, 2021.
- [3] Mohammad Gheshlaghi Azar, Ian Osband, and Rémi Munos. Minimax regret bounds for reinforcement learning. In *International Conference on Machine Learning*, 2017.
- [4] Chenjia Bai, Lingxiao Wang, Zhuoran Yang, Zhi-Hong Deng, Animesh Garg, Peng Liu, and Zhaoran Wang. Pessimistic bootstrapping for uncertainty-driven offline reinforcement learning. In *International Conference on Learning Representations*, 2022.
- [5] Tamer Başar and Pierre Bernhard. *H-infinity optimal control and related minimax design problems: a dynamic game approach*. Springer Science & Business Media, 2008.
- [6] Vahid Behzadan and Arslan Munir. Vulnerability of deep reinforcement learning to policy induction attacks. In *International Conference on Machine Learning and Data Mining in Pattern Recognition*, pages 262–275. Springer, 2017.
- [7] Jinglin Chen and Nan Jiang. Information-theoretic considerations in batch reinforcement learning. In *International Conference on Machine Learning*, pages 1042–1051. PMLR, 2019.
- [8] Ching-An Cheng, Tengyang Xie, Nan Jiang, and Alekh Agarwal. Adversarially trained actor critic for offline reinforcement learning. *arXiv preprint arXiv:2202.02446*, 2022.
- [9] Adrien Ecoffet, Joost Huizinga, Joel Lehman, Kenneth O Stanley, and Jeff Clune. First return, then explore. *Nature*, 590(7847):580–586, 2021.
- [10] Justin Fu, Aviral Kumar, Ofir Nachum, George Tucker, and Sergey Levine. D4rl: Datasets for deep data-driven reinforcement learning. *arXiv preprint arXiv:2004.07219*, 2020.
- [11] Justin Fu, Aviral Kumar, Ofir Nachum, George Tucker, and Sergey Levine. D4rl: Datasets for deep data-driven reinforcement learning. *arXiv preprint arXiv:2004.07219*, 2020.
- [12] Scott Fujimoto and Shixiang Shane Gu. A minimalist approach to offline reinforcement learning. *Advances in Neural Information Processing Systems*, 34, 2021.
- [13] Scott Fujimoto, David Meger, and Doina Precup. Off-policy deep reinforcement learning without exploration. In *ICML*, 2019.
- [14] Adam Gleave, Michael Dennis, Cody Wild, Neel Kant, Sergey Levine, and Stuart Russell. Adversarial policies: Attacking deep reinforcement learning. In *International Conference on Learning Representations*, 2019.
- [15] Florin Gogianu, Tudor Berariu, Mihaela C Rosca, Claudia Clopath, Lucian Busoniu, and Razvan Pascanu. Spectral normalisation for deep reinforcement learning: an optimisation perspective. In *International Conference on Machine Learning*, pages 3734–3744. PMLR, 2021.
- [16] Ian J Goodfellow, Jonathon Shlens, and Christian Szegedy. Explaining and harnessing adversarial examples. *arXiv preprint arXiv:1412.6572*, 2014.
- [17] Chin Pang Ho, Marek Petrik, and Wolfram Wiesemann. Fast Bellman Updates for Robust MDPs. In *Proceedings of the 35th International Conference on Machine Learning*, pages 1979–1988. PMLR, 2018.
- [18] Sandy Huang, Nicolas Papernot, Ian Goodfellow, Yan Duan, and Pieter Abbeel. Adversarial attacks on neural network policies. *arXiv preprint arXiv:1702.02284*, 2017.

- [19] Garud N Iyengar. Robust dynamic programming. *Mathematics of Operations Research*, 30(2):257–280, 2005.
- [20] Michael Janner, Qiyang Li, and Sergey Levine. Offline reinforcement learning as one big sequence modeling problem. *Advances in neural information processing systems*, 34, 2021.
- [21] Chi Jin, Zhuoran Yang, Zhaoran Wang, and Michael I Jordan. Provably efficient reinforcement learning with linear function approximation. In *Conference on Learning Theory*, pages 2137–2143. PMLR, 2020.
- [22] Ying Jin, Zhuoran Yang, and Zhaoran Wang. Is pessimism provably efficient for offline rl? In *International Conference on Machine Learning*, pages 5084–5096. PMLR, 2021.
- [23] Parameswaran Kamalaruban, Yu-Ting Huang, Ya-Ping Hsieh, Paul Rolland, Cheng Shi, and Volkan Cevher. Robust reinforcement learning via adversarial training with langevin dynamics. *Advances in Neural Information Processing Systems*, 33:8127–8138, 2020.
- [24] Rahul Kidambi, Aravind Rajeswaran, Praneeth Netrapalli, and Thorsten Joachims. Morel: Model-based offline reinforcement learning. In *NeurIPS*, 2020.
- [25] Aviral Kumar, Justin Fu, George Tucker, and Sergey Levine. Stabilizing off-policy q-learning via bootstrapping error reduction. In *NeurIPS*, 2019.
- [26] Aviral Kumar, Aurick Zhou, George Tucker, and Sergey Levine. Conservative q-learning for offline reinforcement learning. In *NeurIPS*, 2020.
- [27] Sergey Levine, Aviral Kumar, George Tucker, and Justin Fu. Offline reinforcement learning: Tutorial, review, and perspectives on open problems. *arXiv preprint arXiv:2005.01643*, 2020.
- [28] Jialian Li, Tongzheng Ren, Dong Yan, Hang Su, and Jun Zhu. Policy learning for robust markov decision process with a mismatched generative model. *arXiv preprint arXiv:2203.06587*, 2022.
- [29] Yuzhe Ma, Xuezhou Zhang, Wen Sun, and Jerry Zhu. Policy poisoning in batch reinforcement learning and control. *Advances in Neural Information Processing Systems*, 32, 2019.
- [30] Bhairav Mehta, Manfred Diaz, Florian Golemo, Christopher J Pal, and Liam Paull. Active domain randomization. In *Conference on Robot Learning*, pages 1162–1176. PMLR, 2020.
- [31] Volodymyr Mnih, Koray Kavukcuoglu, David Silver, Andrei A Rusu, Joel Veness, Marc G Bellemare, Alex Graves, Martin Riedmiller, Andreas K Fidjeland, Georg Ostrovski, et al. Human-level control through deep reinforcement learning. *nature*, 518(7540):529–533, 2015.
- [32] Ashvin Nair, Murtaza Dalal, Abhishek Gupta, and Sergey Levine. Accelerating online reinforcement learning with offline datasets. *arXiv preprint arXiv:2006.09359*, 2020.
- [33] Arnab Nilim and Laurent Ghaoui. Robustness in markov decision problems with uncertain transition matrices. *Advances in neural information processing systems*, 16, 2003.
- [34] Ian Osband, Charles Blundell, Alexander Pritzel, and Benjamin Van Roy. Deep exploration via bootstrapped dqn. In *NeurIPS*, 2016.
- [35] Nicolas Papernot, Patrick McDaniel, Ian Goodfellow, Somesh Jha, Z Berkay Celik, and Ananthram Swami. Practical black-box attacks against deep learning systems using adversarial examples. *arXiv preprint arXiv:1602.02697*, 1(2):3, 2016.
- [36] Anay Pattanaik, Zhenyi Tang, Shuijing Liu, Gautham Bommannan, and Girish Chowdhary. Robust deep reinforcement learning with adversarial attacks. *arXiv preprint arXiv:1712.03632*, 2017.
- [37] Anay Pattanaik, Zhenyi Tang, Shuijing Liu, Gautham Bommannan, and Girish Chowdhary. Robust deep reinforcement learning with adversarial attacks. In *Proceedings of the 17th International Conference on Autonomous Agents and MultiAgent Systems*, pages 2040–2042, 2018.
- [38] Lerrel Pinto, James Davidson, Rahul Sukthankar, and Abhinav Gupta. Robust adversarial reinforcement learning. In *International Conference on Machine Learning*, pages 2817–2826. PMLR, 2017.
- [39] Aravind Rajeswaran, Sarvjeet Ghotra, Balaraman Ravindran, and Sergey Levine. Epopt: Learning robust neural network policies using model ensembles. *arXiv preprint arXiv:1610.01283*, 2016.

- [40] Paria Rashidinejad, Banghua Zhu, Cong Ma, Jiantao Jiao, and Stuart Russell. Bridging offline reinforcement learning and imitation learning: A tale of pessimism. *Advances in Neural Information Processing Systems*, 34, 2021.
- [41] Aurko Roy, Huan Xu, and Sebastian Pokutta. Reinforcement learning under model mismatch. *Advances in neural information processing systems*, 30, 2017.
- [42] Julian Schrittwieser, Ioannis Antonoglou, Thomas Hubert, Karen Simonyan, Laurent Sifre, Simon Schmitt, Arthur Guez, Edward Lockhart, Demis Hassabis, Thore Graepel, et al. Mastering atari, go, chess and shogi by planning with a learned model. *Nature*, 588(7839):604–609, 2020.
- [43] Qianli Shen, Yan Li, Haoming Jiang, Zhaoran Wang, and Tuo Zhao. Deep reinforcement learning with robust and smooth policy. In *International Conference on Machine Learning*, pages 8707–8718. PMLR, 2020.
- [44] David Silver, Aja Huang, Chris J Maddison, Arthur Guez, Laurent Sifre, George Van Den Driessche, Julian Schrittwieser, Ioannis Antonoglou, Veda Panneershelvam, Marc Lanctot, et al. Mastering the game of go with deep neural networks and tree search. *nature*, 529(7587):484–489, 2016.
- [45] Samarth Sinha, Ajay Mandlekar, and Animesh Garg. S4rl: Surprisingly simple self-supervision for offline reinforcement learning in robotics. In *Conference on Robot Learning*, pages 907–917. PMLR, 2022.
- [46] Aviv Tamar, Huan Xu, and Shie Mannor. Scaling up robust mdps by reinforcement learning. *arXiv preprint arXiv:1306.6189*, 2013.
- [47] Michael E Tipping and Christopher M Bishop. Probabilistic principal component analysis. *Journal of the Royal Statistical Society: Series B (Statistical Methodology)*, 61(3):611–622, 1999.
- [48] Josh Tobin, Rachel Fong, Alex Ray, Jonas Schneider, Wojciech Zaremba, and Pieter Abbeel. Domain randomization for transferring deep neural networks from simulation to the real world. In *2017 IEEE/RSJ international conference on intelligent robots and systems (IROS)*, pages 23–30. IEEE, 2017.
- [49] Eugene Vinitsky, Yuqing Du, Kanaad Parvate, Kathy Jang, Pieter Abbeel, and Alexandre Bayen. Robust reinforcement learning using adversarial populations. *arXiv preprint arXiv:2008.01825*, 2020.
- [50] Jianhao Wang, Wenzhe Li, Haozhe Jiang, Guangxiang Zhu, Siyuan Li, and Chongjie Zhang. Offline reinforcement learning with reverse model-based imagination. *Advances in Neural Information Processing Systems*, 34, 2021.
- [51] Qing Wang, Jiechao Xiong, Lei Han, Han Liu, Tong Zhang, et al. Exponentially weighted imitation learning for batched historical data. *Advances in Neural Information Processing Systems*, 31, 2018.
- [52] Ruosong Wang, Simon S Du, Lin F Yang, and Ruslan Salakhutdinov. On reward-free reinforcement learning with linear function approximation. In *Advances in neural information processing systems*, 2020.
- [53] Ziyu Wang, Alexander Novikov, Konrad Zolna, Josh S Merel, Jost Tobias Springenberg, Scott E Reed, Bobak Shahriari, Noah Siegel, Caglar Gulcehre, Nicolas Heess, et al. Critic regularized regression. *Advances in Neural Information Processing Systems*, 33:7768–7778, 2020.
- [54] Fan Wu, Linyi Li, Chejian Xu, Huan Zhang, Bhavya Kailkhura, Krishnaram Kenthapadi, Ding Zhao, and Bo Li. Copa: Certifying robust policies for offline reinforcement learning against poisoning attacks. *arXiv preprint arXiv:2203.08398*, 2022.
- [55] Yifan Wu, George Tucker, and Ofir Nachum. Behavior regularized offline reinforcement learning. *arXiv preprint arXiv:1911.11361*, 2019.
- [56] Lihua Xie and Carlos E de Souza. Robust h/sub infinity/control for linear systems with norm-bounded time-varying uncertainty. In *29th IEEE Conference on Decision and Control*, pages 1034–1035. IEEE, 1990.

- [57] Tengyang Xie, Ching-An Cheng, Nan Jiang, Paul Mineiro, and Alekh Agarwal. Bellman-consistent pessimism for offline reinforcement learning. *Advances in neural information processing systems*, 34, 2021.
- [58] Wenhao Yang, Liangyu Zhang, and Zhihua Zhang. Towards theoretical understandings of robust markov decision processes: Sample complexity and asymptotics. *arXiv preprint arXiv:2105.03863*, 2021.
- [59] Yiqin Yang, Xiaoteng Ma, Li Chenghao, Zewu Zheng, Qiyuan Zhang, Gao Huang, Jun Yang, and Qianchuan Zhao. Believe what you see: Implicit constraint approach for offline multi-agent reinforcement learning. *Advances in Neural Information Processing Systems*, 34, 2021.
- [60] Ming Yin, Yaqi Duan, Mengdi Wang, and Yu-Xiang Wang. Near-optimal offline reinforcement learning with linear representation: Leveraging variance information with pessimism. *arXiv preprint arXiv:2203.05804*, 2022.
- [61] Tianhe Yu, Aviral Kumar, Rafael Rafailov, Aravind Rajeswaran, Sergey Levine, and Chelsea Finn. Combo: Conservative offline model-based policy optimization. *Advances in Neural Information Processing Systems*, 34, 2021.
- [62] Tianhe Yu, Garrett Thomas, Lantao Yu, Stefano Ermon, James Zou, Sergey Levine, Chelsea Finn, and Tengyu Ma. Mopo: Model-based offline policy optimization. In *NeurIPS*, 2020.
- [63] Huan Zhang, Hongge Chen, Chaowei Xiao, Bo Li, Mingyan Liu, Duane Boning, and Chao-Jui Hsieh. Robust deep reinforcement learning against adversarial perturbations on state observations. *Advances in Neural Information Processing Systems*, 33:21024–21037, 2020.
- [64] Xuezhou Zhang, Yiding Chen, Xiaojin Zhu, and Wen Sun. Robust policy gradient against strong data corruption. In *International Conference on Machine Learning*, pages 12391–12401. PMLR, 2021.
- [65] Zhengqing Zhou, Zhengyuan Zhou, Qinxun Bai, Linhai Qiu, Jose Blanchet, and Peter Glynn. Finite-sample regret bound for distributionally robust offline tabular reinforcement learning. In *International Conference on Artificial Intelligence and Statistics*, pages 3331–3339. PMLR, 2021.

## 9 Theoretical Analysis

In this section, we provide detailed theoretical analysis and proofs in linear MDPs [21].

### 9.1 LSVI Solution

In linear MDPs, we assume that the transition dynamics and reward function take the form of

$$\mathbb{P}_t(s_{t+1} | s_t, a_t) = \langle \psi(s_{t+1}), \phi(s_t, a_t) \rangle, \quad r(s_t, a_t) = \theta^\top \phi(s_t, a_t), \quad \forall (s_{t+1}, a_t, s_t) \in \mathcal{S} \times \mathcal{A} \times \mathcal{S}, \quad (10)$$

where the feature embedding  $\phi : \mathcal{S} \times \mathcal{A} \mapsto \mathbb{R}^d$  is known. We further assume that the reward function  $r : \mathcal{S} \times \mathcal{A} \mapsto [0, 1]$  is bounded and the feature is bounded by  $\|\phi\|_2 \leq 1$ .

Given the offline dataset  $\mathcal{D}$ , the parameter  $w_t$  can be solved in the closed-form by following the LSVI algorithm, which minimizes the following loss function,

$$\hat{w}_t = \min_{w \in \mathbb{R}^d} \sum_{i=1}^m (\phi(s_t^i, a_t^i)^\top w - r(s_t^i, a_t^i) - V_{t+1}(s_{t+1}^i))^2 \quad (11)$$

where  $V_{t+1}$  is the estimated value function in the  $(t+1)$ -th step, and  $y_t^i = r(s_t^i, a_t^i) + V_{t+1}(s_{t+1}^i)$  is the target of LSVI. The explicit solution to (11) takes the form of

$$\hat{w}_t = \Lambda_t^{-1} \sum_{i=1}^m \phi(s_t^i, a_t^i) y_t^i, \quad \text{where } \Lambda_t = \sum_{i=1}^m \phi(s_t^i, a_t^i) \phi(s_t^i, a_t^i)^\top \quad (12)$$

### 9.2 RORL Solution

In RORL, since we introduce the conservative smoothing loss and OOD sampling to learn Q value function, the parameter  $\tilde{w}_t$  of RORL can be solved as follows:

$$\begin{aligned} \tilde{w}_t = \min_{w \in \mathbb{R}^d} & \left[ \sum_{i=1}^m (y_t^i - Q_w(s_t^i, a_t^i))^2 + \sum_{i=1}^m \frac{1}{|\mathbb{B}_d(s_t^i, \epsilon)|} \sum_{\hat{s}_t^i \in \mathcal{D}_{\text{ood}}(s_t^i)} (Q_w(s_t^i, a_t^i) - Q_w(\hat{s}_t^i, a_t^i))^2 + \right. \\ & \left. \sum_{(\hat{s}, \hat{a}, \hat{y}) \sim \mathcal{D}_{\text{ood}}} (\hat{y} - Q_w(\hat{s}, \hat{a}))^2 \right], \end{aligned} \quad (13)$$

which is a simplified learning objective for linear MDPs. The first term is the ordinary TD-error, the second term is the Q value smoothing loss, and the third term is the additional OOD-sampling loss. The explicit solution of Eq. (13) takes the following form by following LSVI:

$$\tilde{w}_t = \tilde{\Lambda}_t^{-1} \left( \sum_{i=1}^m \phi(s_t^i, a_t^i) y_t^i + \sum_{(\hat{s}, \hat{a}, \hat{y}) \sim \mathcal{D}_{\text{ood}}} \phi(\hat{s}, \hat{a}) \hat{y} \right), \quad (14)$$

where the covariance matrix  $\tilde{\Lambda}_t$  is defined as

$$\begin{aligned} \tilde{\Lambda}_t = & \sum_{i=1}^m \phi(s_t^i, a_t^i) \phi(s_t^i, a_t^i)^\top + \sum_{(\hat{s}, \hat{a}) \sim \mathcal{D}_{\text{ood}}} \phi(\hat{s}, \hat{a}) \phi(\hat{s}, \hat{a})^\top \\ & + \sum_{i=1}^m \frac{1}{|\mathbb{B}_d(s_t^i, \epsilon)|} \sum_{\hat{s}_t^i \sim \mathcal{D}_{\text{ood}}(s_t^i)} [\phi(\hat{s}_t^i, a_t^i) - \phi(s_t^i, a_t^i)] [\phi(\hat{s}_t^i, a_t^i) - \phi(s_t^i, a_t^i)]^\top. \end{aligned} \quad (15)$$

We denote the first term of Eq. (15) as  $\tilde{\Lambda}_t^{\text{in}}$ , the second term as  $\tilde{\Lambda}_t^{\text{ood}}$ , and the third term as  $\tilde{\Lambda}_t^{\text{ood-diff}}$ .

### 9.3 $\xi$ -Uncertainty Quantifier

**Theorem** (Theorem 1 restate). *Assume  $\exists i \in [1, m]$  the vector group of all  $\hat{s}_t^i \sim \mathcal{D}_{\text{ood}}(s_t^i)$ :  $\{\phi(\hat{s}_t^i, a_t^i) - \phi(s_t^i, a_t^i)\}$  is full rank, then the covariance matrix  $\tilde{\Lambda}_t^{\text{ood-diff}}$  is positive-definite:  $\tilde{\Lambda}_t^{\text{ood-diff}} \succeq \lambda \cdot \mathbf{I}$  where  $\lambda > 0$ .*

*Proof.* For the  $\tilde{\Lambda}_t^{\text{ood\_diff}}$  matrix (i.e., the third part in Eq. (15)), we denote the covariance matrix for a specific  $i$  as  $\Phi_t^i$ . Then we have  $\tilde{\Lambda}_t^{\text{ood\_diff}} = \sum_{i=1}^m \Phi_t^i$ . In the following, we discuss the condition of positive-definiteness of  $\Phi_t^i$ . For the simplicity of notation, we omit the superscript and subscript of  $s_t^i$  and  $a_t^i$  for given  $i$  and  $t$ . Specifically, we define

$$\Phi_t^i = \frac{1}{|\mathbb{B}_d(s_t^i, \epsilon)|} \sum_{\hat{s}_j \sim \mathcal{D}_{\text{ood}}(s)} [\phi(\hat{s}_j, a) - \phi(s, a)] [\phi(\hat{s}_j, a) - \phi(s, a)]^\top,$$

where  $j \in \{1, \dots, N\}$  indicates we sample  $|\mathbb{B}_d(s_t^i, \epsilon)| = N$  perturbed states for each  $s$ . For a nonzero vector  $y \in \mathbb{R}^d$ , we have

$$\begin{aligned} y^\top \Phi_t^i y &= y^\top \left( \frac{1}{N} \sum_{j=1}^N (\phi(\hat{s}_j, a) - \phi(s, a)) (\phi(\hat{s}_j, a) - \phi(s, a))^\top \right) y \\ &= \frac{1}{N} \sum_{j=1}^N y^\top (\phi(\hat{s}_j, a) - \phi(s, a)) (\phi(\hat{s}_j, a) - \phi(s, a))^\top y \\ &= \frac{1}{N} \sum_{j=1}^N \left( (\phi(\hat{s}_j, a) - \phi(s, a))^\top y \right)^2 \geq 0, \end{aligned} \quad (16)$$

where the last inequality follows from the observation that  $(\phi(\hat{s}_j, a) - \phi(s, a))^\top y$  is a scalar. Then  $\Phi_t^i$  is always positive **semi-definite**.

In the following, we denote  $z_j = \phi(\hat{s}_j, a) - \phi(s, a)$ . Then we need to prove that the condition to make  $\Phi_t^i$  positive **definite** is  $\text{rank}[z_1, \dots, z_N] = d$ , where  $d$  is the feature dimensions. Our proof follows contradiction.

In Eq. (16), when  $y^\top \Phi_t^i y = 0$  with a nonzero vector  $y$ , we have  $z_j^\top y = 0$  for all  $j = 1, \dots, N$ . Suppose the set  $\{z_1, \dots, z_N\}$  spans  $\mathbb{R}^d$ , then there exist real numbers  $\{\alpha_1, \dots, \alpha_N\}$  such that  $y = \alpha_1 z_1 + \dots + \alpha_N z_N$ . But we have  $y^\top y = \alpha_1 z_1^\top y + \dots + \alpha_N z_N^\top y = \alpha_1 * 0 + \dots + \alpha_N * 0 = 0$ , yielding that  $y = 0$ , which forms a contradiction.

Hence, if the set  $\{z_1, \dots, z_N\}$  spans  $\mathbb{R}^d$ , then  $\Phi_t^i$  is positive **definite**. This condition is equivalent to  $\text{rank}[z_1, \dots, z_N] = d$ , which concludes our proof.  $\square$

**Remark.** As a special case, when (i) the dimension of states is the same as the feature  $\phi(s, a)$  and  $\phi(s, a) = s$  and (ii) the size of  $\mathbb{B}_d(s_t^i, \epsilon)$  is sufficient, the matrix  $\tilde{\Lambda}_t^{\text{ood\_diff}}$  satisfies:

$$\tilde{\Lambda}_t^{\text{ood\_diff}} = \sum_{i=1}^m \frac{1}{|\mathbb{B}_d(s_t^i, \epsilon)|} \sum_{\hat{s}_t^i \sim \mathbb{B}_d(s_t^i, \epsilon)} (\hat{s}_t^i - s_t^i)(\hat{s}_t^i - s_t^i)^\top \succeq \frac{m\epsilon^2}{3} \cdot \mathbf{I}.$$

When we use neural networks as the feature extractor, the assumption in Theorem 9.3 needs (i) the size of samples  $\mathbb{B}_d(s_t^i, \epsilon)$  is sufficient, and (ii) the neural network maintains useful variability for state-action features. To obtain the second constraint, we require that the Jacobian matrix of  $\phi(s, a)$  has full rank. Nevertheless, when we use a network as the feature embedding, such a condition can generally be met since the neural network has high randomness and nonlinearity, which results in the feature embedding with sufficient variability. Generally, we only need to enforce a bi-Lipschitz continuity for the feature embedding. We denote  $x_1 = (s_1, a)$  and  $x_2 = (s_2, a)$  as two different inputs.  $x_1^k$  is  $k$ -th dimension of  $x_1$ . The bi-Lipschitz constraint can be formed as

$$C_1 \|x_1^k - x_2^k\|_{\mathcal{X}} \leq \|\phi(x_1) - \phi(x_2)\|_{\Phi} \leq C_2 \|x_1^k - x_2^k\|_{\mathcal{X}}, \quad \forall k \in (1, |\mathcal{X}|), \quad (17)$$

where  $C_1 < C_2$  are two positive constants. The lower-bound  $C_1$  ensures the features space has enough variability for perturbed states, and the upper-bound can be obtained by Spectral regularization [15] that makes the network easy to coverage. An approach to obtain bi-Lipschitz continuity is to regularize the norm of the gradients by using the gradient penalty as

$$\mathcal{L}_{\text{bilip}} = \mathbb{E}_x \left[ \left( \min (\|\nabla_{x^k} \phi(x)\| - C_1, 0) \right)^2 + \left( \max (\|\nabla_{x^k} \phi(x)\| - C_2, 0) \right)^2 \right], \quad \forall k \in (1, |\mathcal{X}|).$$

In experiments, we do not use explicit constraints (e.g., Spectral regularization) for the upper bound since the state has relatively low dimensions, and we find a small fully connected network does not resulting in a large  $C_2$  empirically.

Recall the covariance matrix of PBRL is  $\tilde{\Lambda}_t^{\text{PBRL}} = \tilde{\Lambda}_t^{\text{in}} + \tilde{\Lambda}_t^{\text{ood}}$ , and RORL has a covariance matrix as  $\tilde{\Lambda}_t = \tilde{\Lambda}_t^{\text{PBRL}} + \tilde{\Lambda}_t^{\text{ood\_diff}}$ , we have the following corollary based on Theorem 9.3.

**Corollary** (Corollary 1 restate). *Under the linear MDP assumptions, we have  $\tilde{\Lambda}_t \succeq \tilde{\Lambda}_t^{\text{PBRL}}$ . Further, the covariance matrix  $\tilde{\Lambda}_t$  of RORL is positive-definite:  $\tilde{\Lambda}_t \succeq \lambda \cdot \mathbf{I}$ , where  $\lambda > 0$ .*

Recent theoretical analysis shows that an appropriate uncertainty quantification is essential to provable efficiency in offline RL [22, 57, 4]. Pessimistic Value Iteration [22] defines a general  $\xi$ -uncertainty quantifier as the penalty and achieves provable efficient pessimism in offline RL. We give the definition of a  $\xi$ -uncertainty quantifier as follows.

**Definition 1** ( $\xi$ -Uncertainty Quantifier [22]). *The set of penalization  $\{\Gamma_t\}_{t \in [T]}$  forms a  $\xi$ -Uncertainty Quantifier if it holds with probability at least  $1 - \xi$  that*

$$|\hat{\mathcal{T}}V_{t+1}(s, a) - \mathcal{T}V_{t+1}(s, a)| \leq \Gamma_t(s, a)$$

for all  $(s, a) \in \mathcal{S} \times \mathcal{A}$ , where  $\mathcal{T}$  is the Bellman operator and  $\hat{\mathcal{T}}$  is the empirical Bellman operator that estimates  $\mathcal{T}$  based on the data.

In linear MDPs, Lower Confidence Bound (LCB)-penalty [1, 21] is known to be a  $\xi$ -uncertainty quantifier for appropriately selected  $\beta_t$  as  $\Gamma_t^{\text{LCB}}(s_t, a_t) = \beta_t \cdot [\phi(s_t, a_t)^\top \Lambda_t^{-1} \phi(s_t, a_t)]^{1/2}$ . Following the analysis of PBRL [4], since the bootstrapped uncertainty is an estimation to the LCB-penalty and the OOD sampling provides a covariance matrix of  $\tilde{\Lambda}_t^{\text{PBRL}}$ , the proposed RORL also form a valid  $\xi$ -uncertainty quantifier with the covariance matrix  $\tilde{\Lambda}_t \succeq \lambda \cdot \mathbf{I}$  given in Corollary 9.3.

**Theorem 2.** *For all the OOD datapoint  $(\hat{s}, \hat{a}, \hat{y}) \in \mathcal{D}_{\text{ood}}$ , if we set  $\hat{y} = \mathcal{T}V_{t+1}(s^{\text{ood}}, a^{\text{ood}})$ , it then holds for  $\beta_t = \mathcal{O}(T \cdot \sqrt{d} \cdot \log(T/\xi))$  that*

$$\Gamma_t^{\text{LCB}}(s_t, a_t) = \beta_t [\phi(s_t, a_t)^\top \tilde{\Lambda}_t^{-1} \phi(s_t, a_t)]^{1/2} \quad (18)$$

forms a valid  $\xi$ -uncertainty quantifier, where  $\tilde{\Lambda}_t$  is the covariance matrix of RORL.

*Proof.* The proof follows that of the analysis of PBRL [4] in linear MDPs [22]. We define the empirical Bellman operator of RORL as  $\tilde{\mathcal{T}}$ , then

$$\tilde{\mathcal{T}}V_{t+1}(s_t, a_t) = \phi(s_t, a_t)^\top \tilde{w}_t,$$

where  $\tilde{w}_t$  follows the solution in Eq. (14). Then it suffices to upper bound the following difference between the empirical Bellman operator and Bellman operator

$$\mathcal{T}V_{t+1}(s, a) - \tilde{\mathcal{T}}V_{t+1}(s, a) = \phi(s, a)^\top (w_t - \tilde{w}_t).$$

Here we define  $w_t$  as follows

$$w_t = \theta + \int_{\mathcal{S}} V_{t+1}(s_{t+1}) \psi(s_{t+1}) ds_{t+1}, \quad (19)$$

where  $\theta$  and  $\psi$  are defined in Eq. (10). It then holds that

$$\begin{aligned} \mathcal{T}V_{t+1}(s, a) - \tilde{\mathcal{T}}V_{t+1}(s, a) &= \phi(s, a)^\top (w_t - \tilde{w}_t) \\ &= \phi(s, a)^\top w_t - \phi(s, a)^\top \tilde{\Lambda}_t^{-1} \sum_{i=1}^m \phi(s_t^i, a_t^i) (r(s_t^i, a_t^i) + V_{t+1}^i(s_{t+1}^i)) \\ &\quad - \phi(s, a)^\top \tilde{\Lambda}_t^{-1} \sum_{(\hat{s}, \hat{a}, \hat{y}) \in \mathcal{D}_{\text{ood}}} \phi(\hat{s}, \hat{a}) \hat{y}. \end{aligned} \quad (20)$$



where we plug the solution of  $\tilde{w}_t$  in Eq. (14). Meanwhile, by the definitions of  $\tilde{\Lambda}_t$  and  $w_t$  in Eq. (15) and Eq. (19), respectively, we have

$$\begin{aligned}\phi(s, a)^\top w_t &= \phi(s, a)^\top \tilde{\Lambda}_t^{-1} \tilde{\Lambda}_t w_t \\ &= \phi(s, a)^\top \tilde{\Lambda}_t^{-1} \left( \sum_{i=1}^m \phi(s_t^i, a_t^i) \mathcal{T}V_{t+1}(s_t, a_t) + \sum_{(\hat{s}, \hat{a}, \hat{y}) \in \mathcal{D}_{\text{ood}}} \phi(\hat{s}, \hat{a}) \mathcal{T}V_{t+1}(\hat{s}, \hat{a}) + \right. \\ &\quad \left. \sum_{i=1}^m \frac{1}{|\mathbb{B}_d(s_t^i, \epsilon)|} \sum_{\hat{s}_t^i \sim \mathcal{D}_{\text{ood}}(s_t^i)} [\phi(\hat{s}_t^i, a_t^i) - \phi(s_t^i, a_t^i)] [\phi(\hat{s}_t^i, a_t^i) - \phi(s_t^i, a_t^i)]^\top w_t \right).\end{aligned}\quad (21)$$

Plugging Eq. (21) into Eq. (20) yields

$$\mathcal{T}V_{t+1}(s, a) - \tilde{\mathcal{T}}V_{t+1}(s, a) = \text{(i)} + \text{(ii)} + \text{(iii)}, \quad (22)$$

where we define

$$\begin{aligned}\text{(i)} &= \phi(s, a)^\top \tilde{\Lambda}_t^{-1} \sum_{i=1}^m \phi(s_t^i, a_t^i) (\mathcal{T}V_{t+1}(s_t^i, a_t^i) - r(s_t^i, a_t^i) - V_{t+1}^i(s_{t+1}^i)), \\ \text{(ii)} &= \phi(s, a)^\top \tilde{\Lambda}_t^{-1} \sum_{(\hat{s}, \hat{a}, \hat{y}) \in \mathcal{D}_{\text{ood}}} \phi(\hat{s}, \hat{a}) (\mathcal{T}V_{t+1}(\hat{s}, \hat{a}) - \hat{y}), \\ \text{(iii)} &= \phi(s, a)^\top \tilde{\Lambda}_t^{-1} \sum_{i=1}^m \frac{1}{|\mathbb{B}_d(s_t^i, \epsilon)|} \sum_{\hat{s}_t^i \sim \mathcal{D}_{\text{ood}}(s_t^i)} \left[ \left( \phi(\hat{s}_t^i, a_t^i) \phi(s_t^i, a_t^i)^\top w_t - \phi(s_t^i, a_t^i) \phi(\hat{s}_t^i, a_t^i)^\top w_t \right) \right. \\ &\quad \left. + \left( \phi(s_t^i, a_t^i) \phi(s_t^i, a_t^i)^\top w_t - \phi(s_t^i, a_t^i) \phi(\hat{s}_t^i, a_t^i)^\top w_t \right) \right].\end{aligned}$$

Following the standard analysis based on the concentration of self-normalized process [1, 3, 52, 21, 22] and the fact that  $\Lambda_{\text{ood}} \succeq \lambda \cdot I$ , it holds that

$$|\text{(i)}| \leq \beta_t \cdot [\phi(s_t, a_t)^\top \Lambda_t^{-1} \phi(s_t, a_t)]^{1/2}, \quad (23)$$

with probability at least  $1 - \xi$ , where  $\beta_t = \mathcal{O}(T \cdot \sqrt{d} \cdot \log(T/\xi))$ . Meanwhile, by setting  $y = \mathcal{T}V_{t+1}(s^{\text{ood}}, a^{\text{ood}})$ , it holds that  $\text{(ii)} = 0$ . For  $\text{(iii)}$ , we have

$$\begin{aligned}& \left( \phi(\hat{s}_t^i, a_t^i) \phi(s_t^i, a_t^i)^\top w_t - \phi(s_t^i, a_t^i) \phi(\hat{s}_t^i, a_t^i)^\top w_t \right) + \left( \phi(s_t^i, a_t^i) \phi(s_t^i, a_t^i)^\top w_t - \phi(s_t^i, a_t^i) \phi(\hat{s}_t^i, a_t^i)^\top w_t \right) \\ &= \phi(\hat{s}_t^i, a_t^i) \left( \mathcal{T}V_{t+1}(\hat{s}_t^i, a_t^i) - \mathcal{T}V_{t+1}(s_t^i, a_t^i) \right) + \phi(s_t^i, a_t^i) \left( \mathcal{T}V_{t+1}(s_t^i, a_t^i) - \mathcal{T}V_{t+1}(\hat{s}_t^i, a_t^i) \right) \\ &= (\phi(\hat{s}_t^i, a_t^i) - \phi(s_t^i, a_t^i)) (\mathcal{T}V_{t+1}(\hat{s}_t^i, a_t^i) - \mathcal{T}V_{t+1}(s_t^i, a_t^i))\end{aligned}\quad (24)$$

Since we enforce smoothness for the value function, we have  $\mathcal{T}V_{t+1}(\hat{s}_t^i, a_t^i) \approx \mathcal{T}V_{t+1}(s_t^i, a_t^i)$ . Thus  $\text{(iii)} \approx 0$ . To conclude, we obtain from Eq. (22) that

$$|\mathcal{T}V_{t+1}(s, a) - \tilde{\mathcal{T}}V_{t+1}(s, a)| \leq \beta_t \cdot [\phi(s_t, a_t)^\top \Lambda_t^{-1} \phi(s_t, a_t)]^{1/2} \quad (25)$$

for all  $(s, a) \in \mathcal{S} \times \mathcal{A}$  with probability at least  $1 - \xi$ .  $\square$

## 9.4 Suboptimality Gap

Theorem 2 allows us to further characterize the optimality gap based on the pessimistic value iteration [22]. First, we give the following lemma.

**Lemma 1.** *Given two positive definite matrix  $A$  and  $B$ , it holds that:*

$$\frac{x^\top A^{-1} x}{x^\top (A + B)^{-1} x} > 1. \quad (26)$$

*Proof.* Leveraging the properties of generalized Rayleigh quotient, we have

$$\frac{x^\top A^{-1} x}{x^\top (A + B)^{-1} x} \geq \lambda_{\min}((A + B)A^{-1}) = \lambda_{\min}(I + BA^{-1}) = 1 + \lambda_{\min}(BA^{-1}). \quad (27)$$

Since  $B$  and  $A^{-1}$  are both positive definite, the eigenvalues of  $BA^{-1}$  are all positive:  $\lambda_{\min}(BA^{-1}) > 0$ . This ends the proof.  $\square$

Then, according to the definition of LCB-penalty in Eq. (18), since  $\tilde{\Lambda}_t = \tilde{\Lambda}_t^{\text{PBRL}} + \tilde{\Lambda}_t^{\text{ood\_diff}}$  with  $\tilde{\Lambda}_t^{\text{ood\_diff}} \succeq \lambda I$ , we have the relationship of the LCB-penalty between RORL and PBRL as follows.

**Corollary 3.** *The RORL-induced LCB-penalty term is less than the PBRL-induced LCB-penalty, as  $\Gamma_t^{\text{lc}}(s_t, a_t) = \beta_t [\phi(s_t, a_t)^\top \tilde{\Lambda}_t^{-1} \phi(s_t, a_t)]^{1/2} < \Gamma_t^{\text{lc\_PBRL}}(s_t, a_t)$ .*

*Proof.* Since  $\tilde{\Lambda}_t = \tilde{\Lambda}_t^{\text{PBRL}} + \tilde{\Lambda}_t^{\text{ood\_diff}}$  and  $\tilde{\Lambda}_t^{\text{ood\_diff}} \succeq \lambda I$ , we have

$$\frac{\phi(s_t, a_t)^\top \tilde{\Lambda}_t^{-1} \phi(s_t, a_t)}{\phi(s_t, a_t)^\top (\tilde{\Lambda}_t^{\text{PBRL}})^{-1} \phi(s_t, a_t)} = \frac{\phi(s_t, a_t)^\top (\tilde{\Lambda}_t^{\text{PBRL}} + \tilde{\Lambda}_t^{\text{ood\_diff}})^{-1} \phi(s_t, a_t)}{\phi(s_t, a_t)^\top (\tilde{\Lambda}_t^{\text{PBRL}})^{-1} \phi(s_t, a_t)} < 1. \quad (28)$$

where the inequality directly follows Lemma 1. Then we have

$$\phi(s_t, a_t)^\top \tilde{\Lambda}_t^{-1} \phi(s_t, a_t) < \phi(s_t, a_t)^\top (\tilde{\Lambda}_t^{\text{PBRL}})^{-1} \phi(s_t, a_t). \quad (29)$$

□

Theorem 2 and Corollary 3 allow us to further characterize the optimality gap of the pessimistic value iteration. In particular, we have the following suboptimality gap under linear MDP assumptions.

**Corollary** (Corollary 2 restate). *Under the same conditions as Theorem 2, it holds that  $\text{SubOpt}(\pi^*, \hat{\pi}) \leq \sum_{t=1}^T \mathbb{E}_{\pi^*} [\Gamma_t^{\text{lc}}(s_t, a_t)] < \sum_{t=1}^T \mathbb{E}_{\pi^*} [\Gamma_t^{\text{lc\_PBRL}}(s_t, a_t)]$ .*

We refer to Jin et al [22] for a detailed proof of the first inequality. The second inequality is directly induced by  $\Gamma_t^{\text{lc}}(s_t, a_t) < \Gamma_t^{\text{lc\_PBRL}}(s_t, a_t)$  in Corollary 3. The optimality gap is information-theoretically optimal under the linear MDP setup with finite horizon [22]. Therefore, RORL enjoys a tighter suboptimality bound than PBRL [4] in linear MDPs.

## 10 Implementation Details and Experimental Settings

In this section, we provide detailed implementation and experimental settings.

### 10.1 Implementation Details

#### 10.1.1 SAC-10

Our SAC-10 implementation is based on rlkit<sup>2</sup>, which is open-source and also used by prior works [2, 26, 4]. We keep the default parameters as EDAC [2] except for the ensemble size set to 10 in our paper. In addition, we normalize each dimension of observations in every dataset to a standard normal distribution for consistency with RORL. The hyperparameters are listed in Table 2.

Table 2: Hyper-parameters of SAC-10

Hyper-parameters	Value
The number of bootstrapped networks $K$	10
Policy network	FC(256,256,256) with ReLU activations
Q-network	FC(256,256,256) with ReLU activations
Target network smoothing coefficient $\tau$ for every training step	5e-3
Discount factor $\gamma$	0.99
Policy learning rate	3e-4
Q network learning rate	3e-4
Optimizer	Adam
Automatic Entropy Tuning	True
batch size	256

<sup>2</sup><https://github.com/vitchyr/rlkit>

### 10.1.2 EDAC

Our EDAC implementation is based on the open-source code of the original paper [2]. In the benchmark results, we directly report results from the paper which are the previous SOTA performance on the Gym benchmark. As for other experiments, we also normalize the observations and use 10 ensemble  $Q$  networks for consistency with RORL, and set the gradient diversity term  $\eta = 1$ .

### 10.1.3 RORL

We implement RORL based on SAC-10 and keep the hyperparameters the same. The differences are the introduced policy and  $Q$  network smoothing techniques and the additional value underestimation on OOD state-action pairs. In Eq. (5), the coefficient  $\alpha$  for the  $Q$  network smoothing loss  $\mathcal{L}_{\text{smooth}}$  is set to 0.0001 for all tasks, and the coefficient  $\beta$  for the OOD loss  $\mathcal{L}_{\text{ood}}$  is tuned within  $\{0.0, 0.1, 0.5\}$ . Besides, the coefficient  $\alpha_2$  of the policy smoothing loss in Eq. (6) is searched in  $\{0.1, 1.0\}$ . When training the policy and value functions in RORL, we randomly sample  $n$  perturbed observations from a  $l_\infty$  ball of norm  $\epsilon$  and select the one that maximizes  $D_{\mathcal{J}}(\pi_\theta(\cdot|s) \parallel \pi_\theta(\cdot|\hat{s}))$  and  $\mathcal{L}_{\text{smooth}}$ , respectively. We denote the perturbation scales for the  $Q$  value functions, the policy, and the OOD loss as  $\epsilon_Q$ ,  $\epsilon_P$  and  $\epsilon_{\text{ood}}$ . The number of sampled perturbed observations  $n$  is tuned within  $\{10, 20, 30, 40\}$ . The OOD loss underestimates the values for  $n$  perturbed states  $\hat{s} \sim \mathbb{B}_d(s, \epsilon)$  with actions sampled from the current policy  $\hat{a} \sim \pi_\theta(\hat{s})$ . Regarding the  $Q$  smoothing loss in Eq. (3), the parameter  $\tau$  is set to 0.2 in all tasks for conservative value estimation. All the hyper-parameters used in RORL for the benchmark and adversarial experiments are listed in Table 3 and Table 4 respectively. Note that for halfcheetah tasks, 10 ensemble  $Q$  networks already enforce sufficient pessimism for OOD state-action pairs, thus we do not need additional OOD loss for these tasks.

As for the OOD loss  $\mathcal{L}_{\text{ood}}$  in Eq. (4), we remark that the pseudo-target  $\hat{\mathcal{T}}_{\text{ood}} Q_{\phi_i}(\hat{s}, \hat{a})$  for the OOD state-action pairs  $(\hat{s}, \hat{a})$  can be implemented in two ways:  $\hat{\mathcal{T}}_{\text{ood}} Q_{\phi_i}(\hat{s}, \hat{a}) := Q_{\phi_i}(\hat{s}, \hat{a}) - \lambda u(\hat{s}, \hat{a})$  and  $\hat{\mathcal{T}}_{\text{ood}} Q_{\phi_i}(\hat{s}, \hat{a}) := \min_{i=1, \dots, K} Q_{\phi_i}(\hat{s}, \hat{a})$ . We refer to the two targets as the “minus target” and the “min target”, and compare them in Appendix 11.2. Intuitively, the “minus target” introduces an additional parameter  $\lambda$  but is more flexible to tune for different tasks and different types of data. In contrast, the “min target” requires tuning the number of ensemble  $Q$  networks and cannot enforce appropriate conservatism for all tasks given 10 ensemble  $Q$  networks. Following PBRL [4], we also decay the OOD regularization coefficient  $\lambda$  with decay pace  $d$  for each training step to stabilize  $\mathcal{L}_{\text{ood}}$  since we need strong OOD regularization at the beginning of training and need to avoid too large OOD loss that leads the value function to be fully negative.  $\lambda$  and  $d$  are also listed in the two tables.

Table 3: Hyper-parameters of RORL for the benchmark results

Task Name	$\alpha$	$\alpha_2$	$\beta$	$\epsilon_Q$	$\epsilon_P$	$\epsilon_{\text{ood}}$	$\tau$	$n$	$\lambda (d)$
halfcheetah-random	0.0001	1.0	0.0	0.005	0.005	0.00	0.2	30	0
halfcheetah-medium				0.001	0.001			10	
halfcheetah-medium-expert				0.001	0.001			10	
halfcheetah-medium-replay				0.001	0.001			10	
hopper-random	0.0001	0.1	0.5	0.005	0.005	0.05	0.2	30	$1 \rightarrow 0.1 (1e^{-6})$
hopper-medium		0.1				0.05		40	$1 \rightarrow 0.1 (1e^{-6})$
hopper-medium-expert		0.1				0.03		40	$2 \rightarrow 0.7 (3e^{-6})$
hopper-medium-replay		1.0				0.05		30	$1 \rightarrow 0.1 (1e^{-6})$
walker2d-random	0.0001	0.1	0.5	0.005	0.005	0.01	0.2	20	$5 \rightarrow 0.5 (1e^{-5})$
walker2d-medium		1.0	0.1	0.01	0.01				$1 \rightarrow 0.1 (1e^{-6})$
walker2d-medium-expert		1.0	0.1	0.01	0.01				$1 \rightarrow 0.1 (1e^{-6})$
walker2d-medium-replay		1.0	0.1	0.01	0.01				$1 \rightarrow 0.1 (1e^{-6})$

Table 4: Hyper-parameters of RORL for the adversarial attack results

Task Name	$\alpha$	$\alpha_2$	$\beta$	$\epsilon_Q$	$\epsilon_P$	$\epsilon_{\text{ood}}$	$\tau$	$n$	$\lambda (d)$
halfcheetah-medium	0.0001	1.0	0.0	0.05	0.1	0.00	0.2	30	0
walker2d-medium			0.5	0.03		0.05			$1 \rightarrow 0.1 (1e^{-6})$

## 10.2 Experimental Settings

For all experiments, we run algorithms for 3000 epochs (1000 training steps each epoch, i.e., 3 million steps in total) following EDAC [2]. We use small perturbation scales to train the  $Q$  networks and the policy network for the benchmark experiments and relatively large scales for the adversarial attack experiments as listed in Table 3 and Table 4.

In the benchmark results, we evaluate algorithms for 1000 steps in clean environments (without adversarial attack) at the end of an epoch. The reported results are normalized to d4rl scores that measure how the performance compared with expert score and random score:  $\text{normalized score} = 100 \times \frac{\text{score} - \text{random score}}{\text{expert score} - \text{random score}}$ . Besides, the benchmark results are averaged over 4 random seeds. Regarding the adversarial attack experiments, we evaluate algorithms in perturbed environments that performing “random”, “action diff”, and “min Q” attack with zero-order and mixed-order optimizers as discussed in Sec 6.2. Similar to prior work [63], agents receive observations with malicious noise and the environments do not change their internal transition dynamics. We evaluate each algorithm for 5 trajectories and average their returns over 3 random seeds.

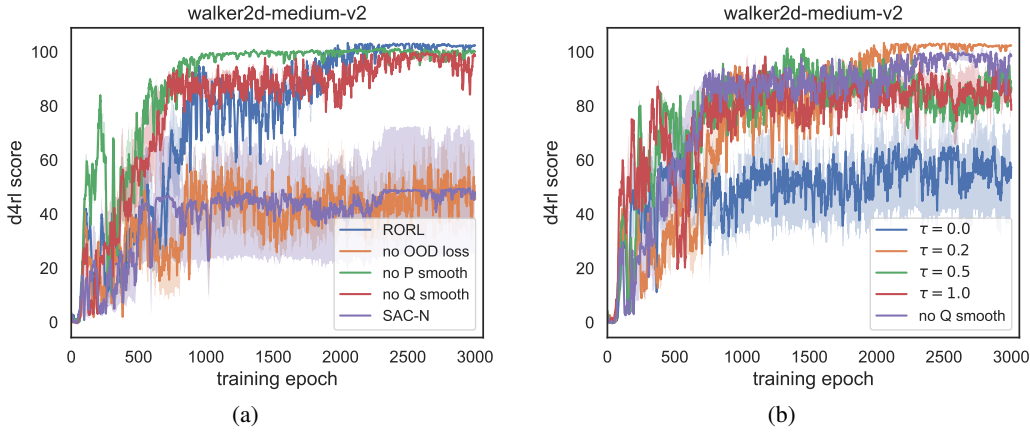


Figure 6: (a) Ablation studies of three introduced loss (the “P smooth” and the “Q smooth” refer to the policy smoothing loss and the Q network smoothing loss), and (b) the hyper-parameter  $\tau$  on the benchmark experiments.

## 11 Additional Experimental Results

In this section, we present additional ablation studies and adversarial experiments.

### 11.1 Ablations on Benchmark Results

In the benchmark results, RORL outperforms other baselines, especially in the walker2d task. We conduct ablation studies on this task to verify the effectiveness of RORL’s components. In Figure 6 (a), we can find that each introduced loss (i.e., the OOD loss, the policy smoothing loss and the Q network smoothing loss) influences the performance on walker2d-medium-v2 task. Specifically, the OOD loss affects the most, without which the performance would drop close to SAC-N’s performance on this task. In addition, the Q smoothing loss is more important for stabilizing the final performance in clean environments than the policy smoothing loss.

In Figure 6 (b), we evaluate the performance of RORL with varying  $\tau$ . The results suggest that  $\tau$  is an important factor that balances the learning of in-distribution and out-of-distribution Q values. In Eq (3), we want to assign larger weights  $(1 - \tau)$  on the  $\delta(s, \hat{s}, a)_+^2$  and smaller weights ( $\tau$ ) on the  $\delta(s, \hat{s}, a)_-^2$  to underestimate the values of OOD states, where  $\delta(s, \hat{s}, a) = Q_{\phi_i}(\hat{s}, a) - Q_{\phi_i}(s, a)$ . On the contrary, a too small  $\tau$  can also lead to overestimation of in-distribution state-action pairs. Further, the in-distribution value estimation is more crucial for clean environments without adversarial noise. In Figure 6 (b),  $\tau = 0$  leads to poor performance while larger  $\tau = 0.5, 1.0$  also result in performance worse than RORL without Q smoothing. Empirically, we find  $\tau = 0.2$  works well for all tasks.

One direction for future improvement is to detach the gradients for the Q values of in-distribution state-action pairs to avoid the potential negative impact.

In the above analysis, we know the OOD loss is a key component in RORL. We further study the impact of the OOD loss and  $\epsilon_{\text{ood}}$  on the performance and the value estimation. As shown in Figure 7 (a), when  $\epsilon_{\text{ood}} = 0$ , the performance of RORL drops significantly, which illustrates the effectiveness of underestimating values of OOD states since the smoothness of RORL may overestimates these values. From Figure 7 (b), we can verify that the OOD loss with  $\epsilon_{\text{ood}} > 0$  contributes to the value underestimation.

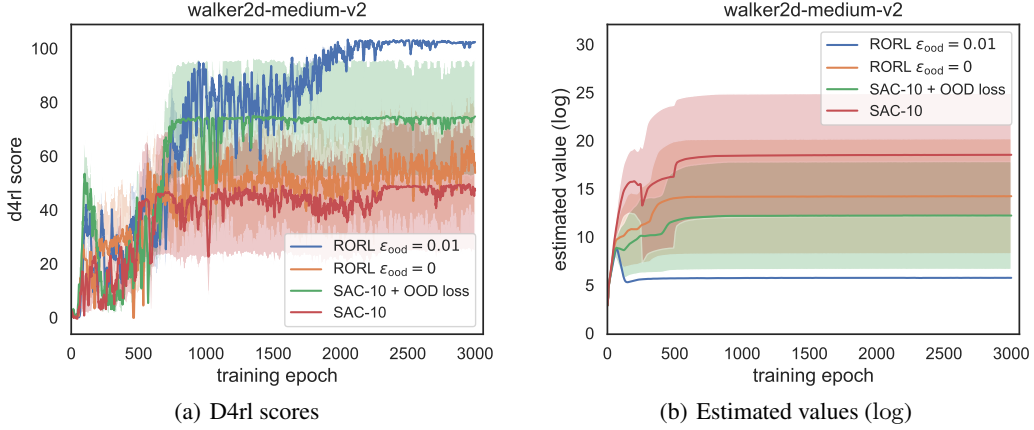


Figure 7: The ablations of the OOD loss  $\mathcal{L}_{\text{ood}}$  and the hyper-parameter  $\epsilon_{\text{ood}}$  on the benchmark experiments.

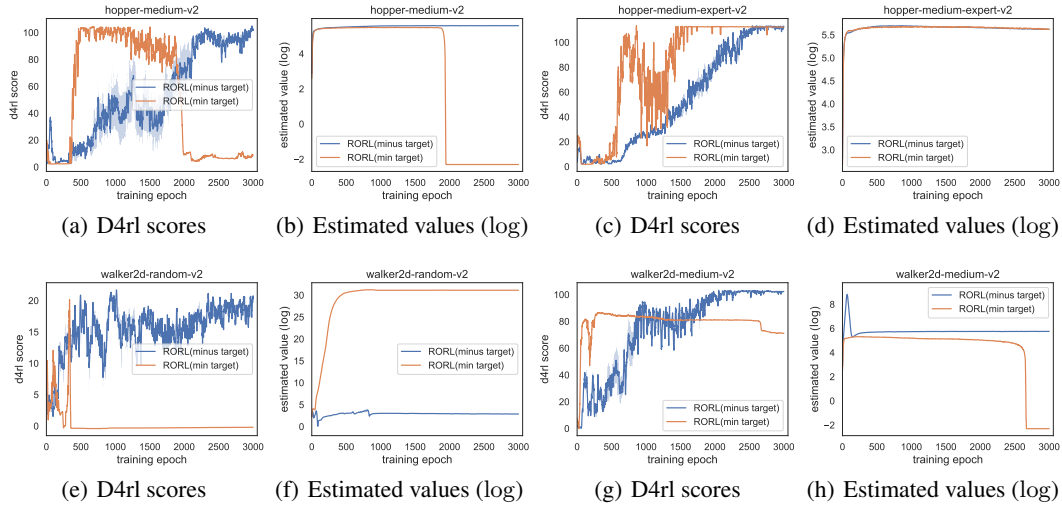


Figure 8: Comparison of the “minus target” and the “min target” in the OOD loss  $\mathcal{L}_{\text{ood}}$  on four tasks.

## 11.2 Comparison of the “minus target” and the “min target”

In the OOD loss  $\mathcal{L}_{\text{ood}}$  (Eq (4)), the pseudo-target  $\hat{\mathcal{T}}_{\text{ood}} Q_{\phi_i}(\hat{s}, \hat{a})$  for the OOD state-action pairs  $(\hat{s}, \hat{a})$  can be implemented in two ways to underestimate the values of  $(\hat{s}, \hat{a})$ :  $\hat{\mathcal{T}}_{\text{ood}} Q_{\phi_i}(\hat{s}, \hat{a}) := Q_{\phi_i}(\hat{s}, \hat{a}) - \lambda u(\hat{s}, \hat{a})$  and  $\hat{\mathcal{T}}_{\text{ood}} Q_{\phi_i}(\hat{s}, \hat{a}) := \min_{i=1, \dots, K} Q_{\phi_i}(\hat{s}, \hat{a})$  ( $K = 10$ ). The two targets are referred to as “minus target” and “min target” respectively. In Figure 8, we compare the two targets’ D4RL scores in clean environments, and the hyper-parameters are the same as the benchmark experiments. Although the “min target” has advantages on the number of hyper-parameters and achieves comparable performance on the hopper-medium-expert-v2 task, it is unstable and not flexible across different tasks, e.g., significantly overestimating values for the walker2d-random-v2 task and

underestimating values for hopper-medium-v2 and walker2d-medium-v2 tasks. Therefore, we choose the “minus target” by default in our paper.

### 11.3 Ablations of $\tau$ for the Adversarial Experiments

In this subsection, we study the performance under adversarial attack with varying  $\tau \in \{0.0, 0.2, 0.5, 1.0\}$ . From the results in Figure 9, we find  $\tau = 0.2$  is the most robust one under “random” and “action diff” attacks. Interestingly, small  $\tau$  (e.g., 0.0 and 0.2) is less robust to “min Q” attack, which might be because the “min Q” attacker has access to both the agent’s Q value functions and policy. Smaller  $\tau$  assists the OOD loss to underestimate OOD values with higher uncertainty, which is helpful for “random” and “action diff” attackers, but it is also easier for the “min Q” attacker to find unfamiliar and dangerous states to attack.

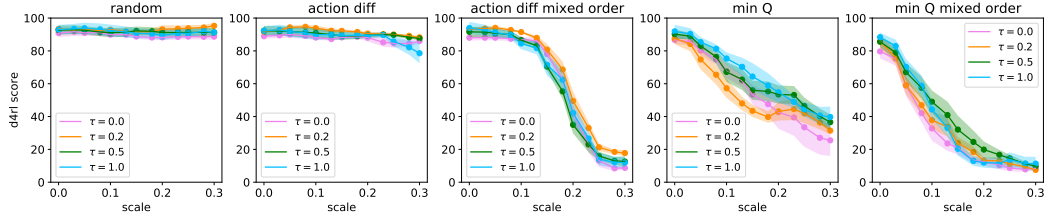


Figure 9: Comparison of different  $\tau$  in the adversarial experiments.

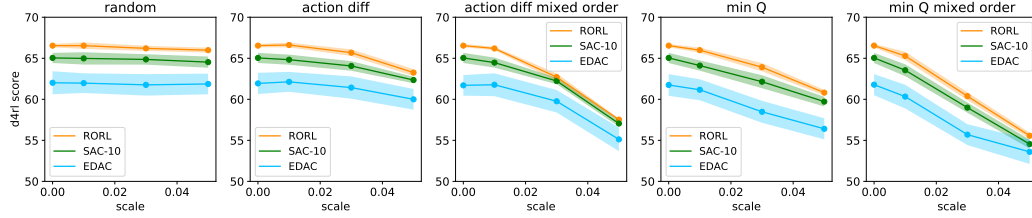
### 11.4 Robustness of the Benchmark Results

In Figure 10, we evaluate RORL’s robustness of the benchmark results, i.e., how robust RORL is to maintain the high performance as listed in Table 1. We compare RORL with EDAC, SAC-10 on six tasks. Note that the EDAC is reproduced with 10 ensemble Q networks as RORL and SAC-10, and uses  $\eta = 1$  for all six tasks. Therefore the performance may be different from that reported in the original paper [2]. The perturbation scales are within range  $\{0.01, 0.03, 0.05\}$  and the results are averaged over 3 random seeds. From the results, we can conclude that RORL can successfully keep the highest performance within a perturbation scale of 0.03 and the performance of EDAC and SAC-10 decreases faster than RORL for most tasks and attack methods. The results imply that RORL has better practicability in real-world scenarios with relatively small perturbations.

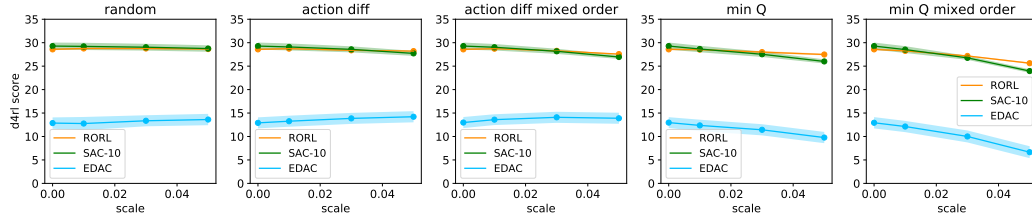
## 12 More Related Works

**Model-Based Offline RL** In offline RL, model-based methods use an empirical model learned from the offline dataset to enhance the generalization ability of offline RL algorithms. The model can be used as the virtual environment for data collecting [62, 24], or augment the dataset then run an existing model-free algorithm [61, 50]. The main challenges of model-based algorithms are how to learn the accurate empirical model and how to construct the uncertainty measure. A recent work [20] demonstrates that the transformer model can generate realistic trajectories, which is enough for policy learning. In contrast, we focus on the model-free methods in this paper and leave the robustness of model-based methods in future work.

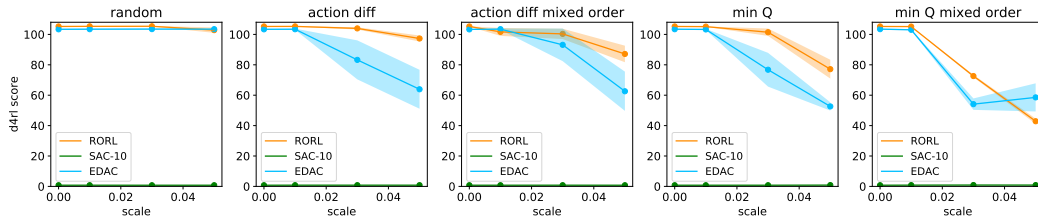
**Adversarial Attack** Inspired by adversarial examples in deep learning [16, 35], adversarial attack and policy poisoning [6, 18, 37] are studied to avoid adversarial manipulations on the network policies. Gleave et al. [14] study adversarial policy in the behavior level [14]. Data corruption [64, 29, 54] considers the case where an attacker can arbitrarily modify the dataset under a specific budget before training. While adversarial attack RL is highly related to robust RL, they focus more on adversarial attacks compared to our robustness setting. More connections between the two topics are something to look forward to in future work.



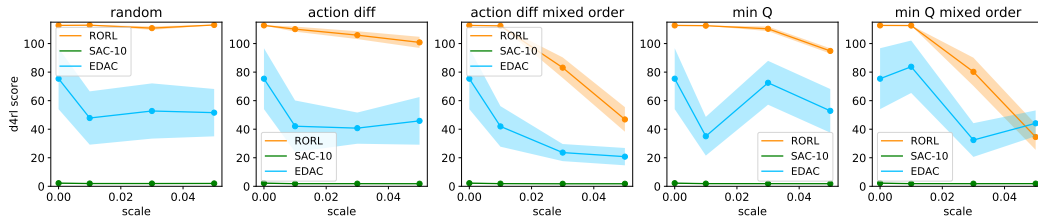
(a) Halfcheetah-medium-v2



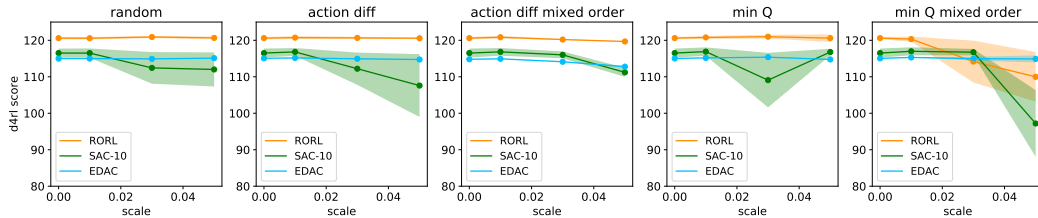
(b) Halfcheetah-random-v2



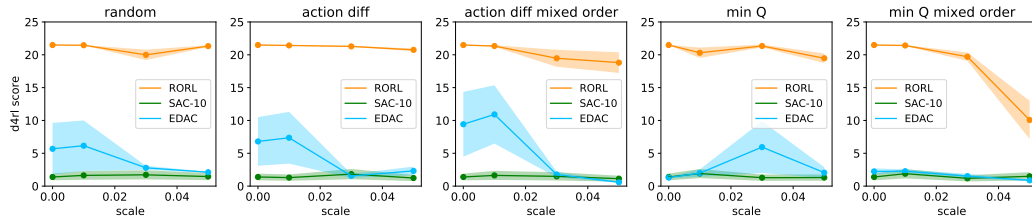
(c) Hopper-medium-v2



(d) Hopper-medium-expert-v2



(e) Walker2d-medium-expert-v2



(f) Walker2d-random-v2

Figure 10: Performance under adversarial attack on six datasets. RORL can maintain the best performance in the benchmark experiments for a certain perturbation scale.